Phase II: Remote mapping of landslides triggered by the July 2021 and August 2022 Marlborough storms, and selected field investigations of landslide impact

BJ Rosser
SL Lin
DB Townsend
A Wolter
J Farr
KE Jones
AF Boyes
E Chen

GNS Science Report 2023/20
July 2023

DISCLAIMER

BIBLIOGRAPHIC REFERENCE

Rosser BJ, Wolter A, Boyes AF, Lin SL, Farr J, Chen E, Townsend DB, Jones KE. 2023. Phase II: Remote mapping of landslides triggered by the July 2021 and August 2022 Marlborough storms, and selected field investigations of landslide impact. Lower Hutt (NZ): GNS Science. 69 p. (GNS Science report; 2023/20). doi:10.21420/5RKR-1618.

BJ Rosser, GNS Science, PO Box 30368, Lower Hutt 5040, New Zealand

A Wolter, GNS Science, PO Box 30368, Lower Hutt 5040, New Zealand

AF Boyes, GNS Science, PO Box 30368, Lower Hutt 5040, New Zealand

SL Lin, GNS Science, PO Box 30368, Lower Hutt 5040, New Zealand

J Farr, GNS Science, PO Box 30368, Lower Hutt 5040, New Zealand

E Chen, Victoria University of Wellington, PO Box 600, Wellington 6140, New Zealand

DB Townsend, GNS Science, PO Box 30368, Lower Hutt 5040, New Zealand

KE Jones, GNS Science, PO Box 30368, Lower Hutt 5040, New Zealand

www.gns.cri.nz

ISSN 2350-3424 (online)
ISBN 978-1-99-105822-5 (online)
http://dx.doi.org/10.21420/5RKR-1618

CONTENTS

FIGURES

TABLES

APPENDICES

APPENDIX TABLES

APPENDIX FIGURES

ABSTRACT

Marlborough has experienced significant storms in the past few years that have triggered widespread and damaging landslides. This report presents an investigation of landslides occurring during the July 2021 and August 2022 storm events. For the July 2021 and August 2022 events, we mapped the distribution of landslides from remote imagery, analysed factors potentially controlling these distributions and sought to explain differences found between the two storms. For the August 2022 storm, we also undertook fieldwork to investigate nine building sites impacted by landslides. We assessed the building damage and related this to the landslide characteristics and also compared these relationships to similar data previously collected for buildings impacted by the July 2021 storm.

Details of the 2021 rainfall event have been summarised in a previous companion report; here, we focus on describing the August 2022 storm. Over 1000 mm of rain fell in some areas during the 2022 storm event, which lasted from the 6th to the 19th of August, 2022. Landslides included mainly debris flows and slides, as well as incipient landsliding (evidenced by ground cracking) and re-activation of relict landslides. Compared to the July 2021 storm, landslides at the investigated building sites tended to be less mobile. Of the nine buildings investigated in detail, three were affected by slippage and six by debris inundation. Damage states (DS) of the buildings investigated ranged from 0 (no damage) to 5 (severe structural damage), with three classified as DS5.

Landslide distributions in July 2021 and August 2022 do not seem to be controlled by the rainfall distribution alone. For both storms, the greatest number and density of landslides did not occur in the areas that received the highest rainfall. Most landslides were shallow and occurred on slopes in weathered schist or semi-schist. In 2021, the highest landslide densities were in harvested forests, and, in 2022, the highest landslide densities were in pasture and regenerating scrub communities.

We recommend more detailed analysis of these datasets, and others, to determine possible landslide trigger thresholds and to conduct risk assessments for vulnerable areas, particularly in the Marlborough Sounds.

KEYWORDS

Marlborough; storm events; July 2021; August 2022; landslide characterisation; landslide distribution; field investigations; RPAS; surveys; land cover; geology

This page left intentionally blank.

1.0 INTRODUCTION AND SCOPE

Marlborough has experienced several significant storms in recent years. We reported on the nature of the July 2021 storm and field investigations of several damaging landslides from the event in Wolter et al. (2022). This report extends that previous work by adding mapping to determine the regional distribution of landslides triggered in the 2021 storm and maps the regional distribution of landslides triggered by the subsequent August 2022 storm, along with reporting on field investigations of several buildings damaged in the August 2022 event. In this report, we compare the landslide distributions and building impacts of these two closely spaced events that affected a very similar area. Details of the 2021 event have been summarised in a previous companion report (Wolter et al. 2022); here, we focus on describing the August 2022 storm.

From the 16th to 19th of August, 2022, an atmospheric river impacted the Nelson and Marlborough regions and delivered extreme rainfall to the top of the South Island. A maximum of 1026 mm was recorded at the Marlborough District Council (MDC) Tunakino rain gauge over four days (a return interval of >250 years, from the High Intensity Rainfall Design System[1]), and some areas in the Marlborough Sounds received between 200 and 800 mm over the four days. Widespread landsliding was triggered by this extreme rainfall event. MDC reported that there were 33 red-stickered houses (uninhabitable) due to landslide damage and that a further 68 houses had been yellow-stickered (Figure 1.1). Dwellings were affected by slippage, where a landslide undermined the building, or were impacted by landslide debris.

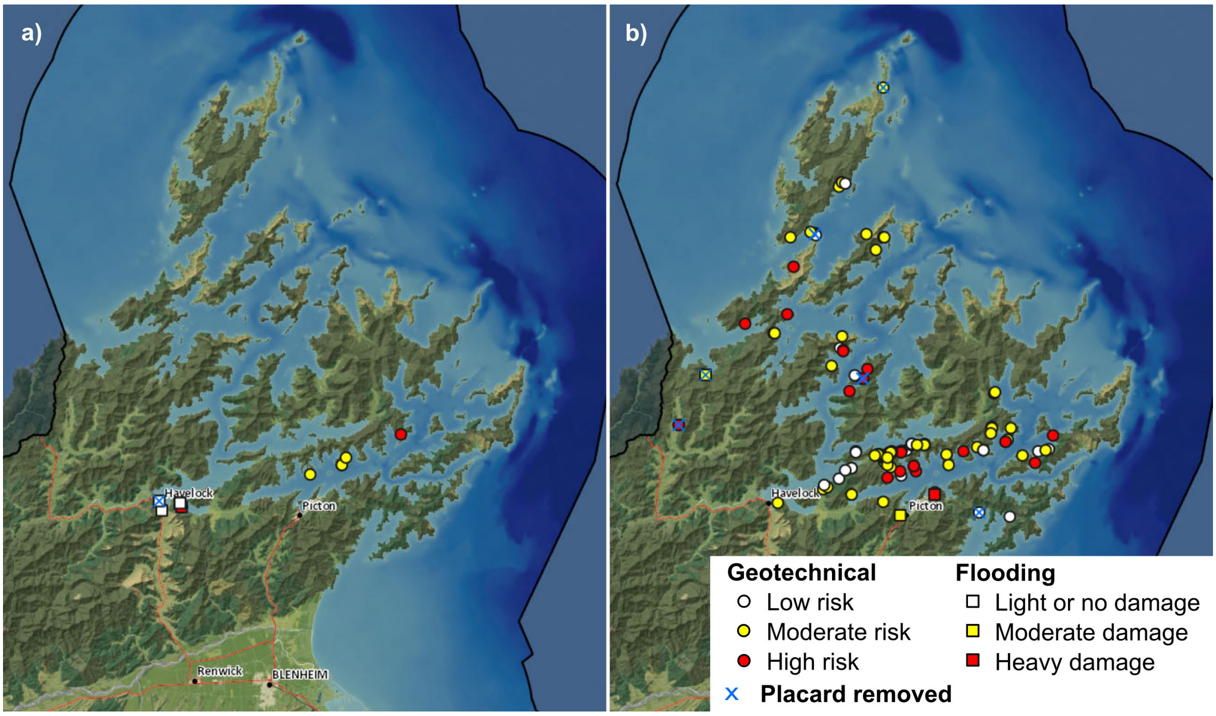

Figure 1.1 Rapid assessments of flood and geotechnical (landslide) damage completed by Marlborough District Council (MDC) after the (a) July 2021 and (b) August 2022 rainfall events. In 2021, three properties were assessed as being at high risk of landslide damage (red, Placard 4 or 5) and six as moderate risk (yellow, Placard 2 or 3). In 2022, 33 properties were deemed to be at high risk and 68 at moderate risk of landslide damage. Placards were removed by MDC after further assessment (source: pers. comm., MDC 2022).

1 https://www.niwa.co.nz/software/hirds

On 20 August 2022, GeoNet, New Zealand's geohazards monitoring agency hosted by GNS Science, initiated a Rapid Landslide Response to the landslide damage in Nelson (Massey et al. 2022). This was expanded to include landslide damage in the Marlborough region after MDC also declared a State of Emergency and requested the assistance of the GNS Science landslide team to assist in their response and recovery to the storm. An aerial reconnaissance flight of the Marlborough Sounds was completed on 7 September 2022 by GNS Science and MDC staff (Rosser et al., in prep). Detailed site visits to nine landslides followed in late September and are summarised in this report.

MDC contracted GNS Science to investigate the landslides triggered by the August 2022 storm event. The scope of work included:

- Improve the spatial and geological understanding of landslides following the August 2022 storm by mapping the landslide distribution from the storm event. In addition, as part of this work, the distribution of landslides produced in the July 2021 storm was also mapped.
- Visit up to 10 residential buildings affected by landslides in the 2022 storm for the purposes of gathering scientific data to inform the GNS Science Landslide Risk Model and to develop fragility functions for landslide damage to buildings. These data will also be used to develop and calibrate the GNS Science Rainfall-Induced Landslide (RIL) forecast tool for the Marlborough region and will be made available to feed into the University of Canterbury Debris Flow Analysis Model.
- Document the size, flow path and downslope impacts of landslides on dwellings in the Marlborough Sounds of the 2022 sites visited for detailed assessments.
- Provide a report (this report) and GIS data (landslide points and polygons, surveys of the site investigations) suitable as inputs to the above models.
- Provide training to MDC staff on landslide documentation methods while in the field.

The project deliverables were:

- A summary of the 2022 storm event.
- Observations from reconnaissance flight and field assessments.
- Regional landslide distributions for the 2021 and 2022 storms.
- Behaviour (landslide type) and mobility (height/length versus landslide volume) of the sites visited for detailed assessments.
- Documentation of impacts to selected properties from the August 2022 storm.

2.0 BACKGROUND INFORMATION

Information on the 16–19 July 2021 storm event (with a maximum rainfall total of 400–500 mm in 54 hours), including descriptions and photographs of the different types and severity of landslides triggered by the July 2021 storm, are provided in Wolter et al. (2022). A summary of observations and photographs from the reconnaissance flight following the August 2022 storm are provided in Rosser et al. (in prep).

Heron (2020) and the Land Cover Database (LCDB) v5 (https://lris.scinfo.org.nz/) should be consulted for a more in-depth summary and maps of the Marlborough geology, textural zones (metamorphic alteration) and land-cover classes.

2.1 2022 Storm Event

Between the 16th and the 19th of August, 2022, the maximum 24-hour rain recorded in the Marlborough District was 390.7 mm (Figure 2.1), and the maximum cumulative amount of rain over the four days was 1026 mm (Figure 2.2). These rainfalls were recorded at the Tunakino rain gauge, located in the Richmond Range.

The National Institute of Water & Atmospheric Research (NIWA)'s High Intensity Rainfall Design System (HIRDS) can estimate high-intensity design rainfall depth at any point in New Zealand, and it is routinely used for assessing storm rarity. The output of HIRDS is a set of tables containing either rainfall depths or rainfall intensities for given storm durations and Annual Recurrence Intervals (ARIs). The ARIs for selected sites in the Marlborough region are shown in Figure 2.3 for the cumulative four-day rainfall depths (shown in Figure 2.2). Although NIWA classified the overall event as being a 1-in-120-year rainfall event for nearby Nelson, the cumulative rainfalls at individual rain gauges in both the Nelson and Marlborough regions had ARIs of >250 years, indicating that the rainfall was severe and rare.

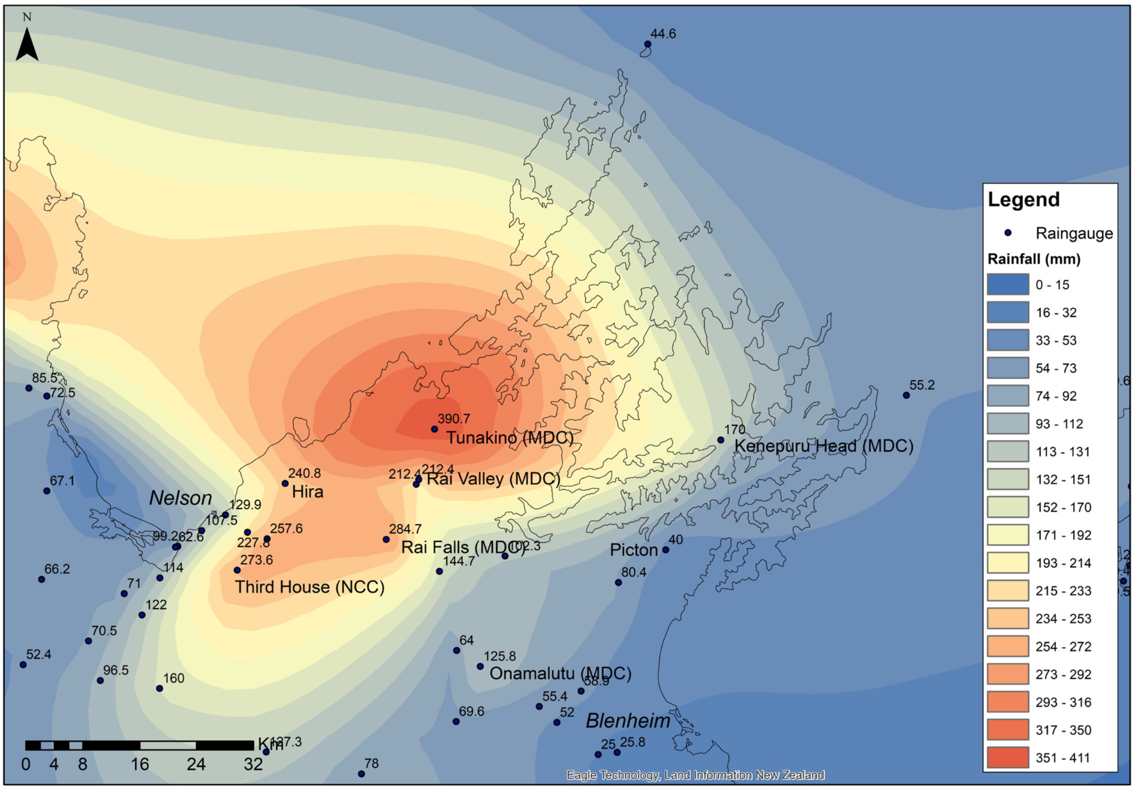

Figure 2.1 Maximum 24-hour rain (depth in millimetres) recorded at rain gauge stations across the Marlborough region within the period 16–19 August 2022.

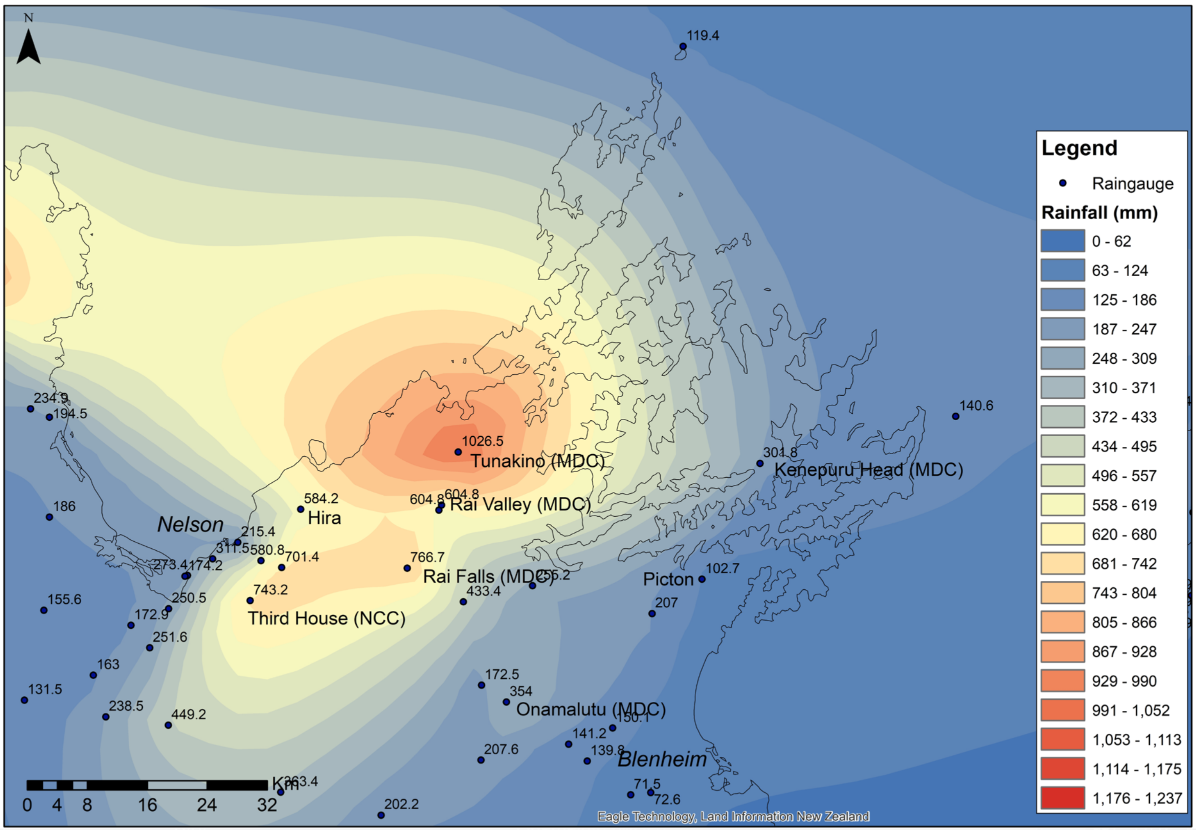

Figure 2.2 Cumulative rain (depth in millimetres) recorded at rain gauge stations across the Marlborough region for the period 16–19 August 2022.

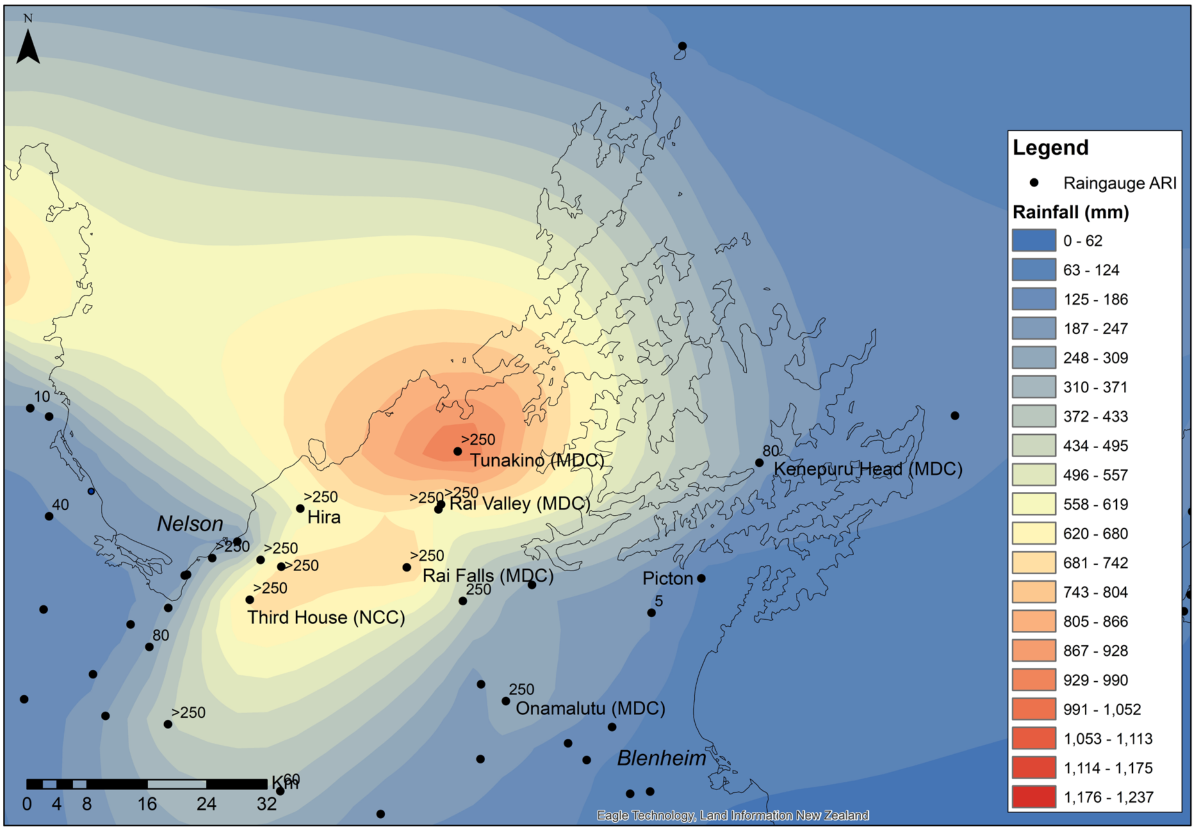

Figure 2.3 Estimated annual recurrence intervals (ARIs) (black labels) for 96-hour rainfall totals for selected rain gauges, from NIWA's High Intensity Rainfall Design System (HIRDS), shown in relation to the cumulative rain (depth in millimetres) across the Marlborough region over the period 16–19 August 2022.

Rainfall totals from gauge-corrected rain radar data (provided by MetService) indicate that some areas of high-intensity rainfall were not recorded by the rain gauge network (Figure 2.4). High rainfall totals were also recorded at D'Urville Island (up to 600 mm) and in the Mount Stokes / Endeavour Inlet area (up to 1000 mm) by the rain radar over the 96-hour storm. Maximum 24-hour rainfall from rain radar was 466 mm in the Bryant Range area, near the Tunakino and Rai Valley stations.

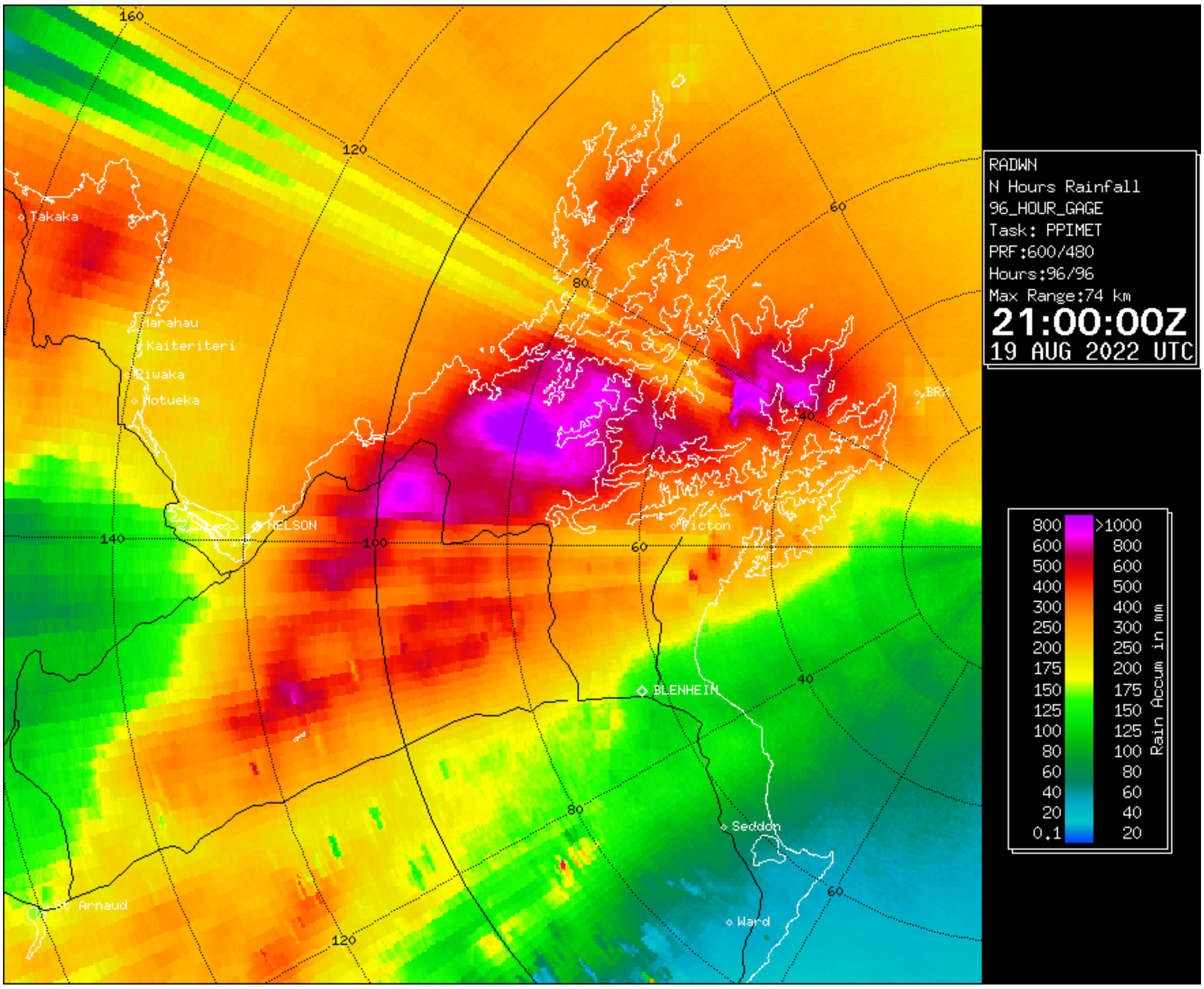

Figure 2.4 Cumulative rain (depth in millimetres) recorded by gauge-corrected rain radar across the Marlborough region for the period 16–19 August 2022 (data provided by MetService).

3.0 LANDSLIDE DISTRIBUTION

3.1 Mapping Methodology and Data Sources

Landslides triggered by the July 2021 and August 2022 storm events were manually mapped using pre- and post-storm aerial photo and satellite imagery to determine the locations of landslides. All landslides, totalling 7597 (3792 in 2021 and 3805 in 2022), were mapped as points, located at the landslide source crown. Of these, 1810 in 2021 and all 3805 in 2022 were also mapped as polygons, representing the landslide source and deposit areas (separately).

The following remote sensing imagery was used to map the landslide distributions for the 2021 and 2022 storm events:

- SkySat 0.5-m-resolution imagery covering the north-eastern portion of the Marlborough Sounds captured on 23 December 2022 and 3 January 2023 (post-August 2022 storm).
- Planet[2] 3-m-resolution imagery covering the Marlborough District, captured on the following dates:
  - Post-July 2021 storm: 7 October 2021.
  - Pre-August 2022 storm: 6, 13 August 2022.
  - Post-August 2022 storm: 29 August; 14, 23 September 2022.
- Sentinel-2 10-m-resolution satellite imagery covering the Marlborough District, captured on the following dates:
  - Pre-July 2021 storm: 23 May; 02, 22, 27, 29 June 2021.
  - Post-July 2021 storm: 30 July; 01, 03 August 2021.
- LINZ 0.3-m-resolution pre-storm 2015–2017 and 2018–2019 aerial photography and summer 2021/22 (partial coverage).
- Land Information New Zealand (LINZ) 2020 1-m-resolution LiDAR elevation data (Digital Elevation Model [DEM] / Digital Surface Model [DSM]), captured by Aerial Surveys between 10 February and 14 August 2020.

3.2 Landslide Inventory Assessment Approach

The landslide points derived from satellite imagery interpretation were overlaid with attribute layers containing key site characteristics in ArcGIS to assess their potential influence in controlling the observed landslide distribution:

- **Slope Angle:** The 8-m-resolution national DEM (LINZ 2012) was used to derive the average slope angle at a mapped landslide site. The 8-m DEM was preferred over the higher-resolution 2020 1 m LiDAR that was available because it better represents the average slope angle of typical slope units and landslide sizes encountered and was consistent with other datasets used in the RIL forecast tool. Slope data were clipped to the study area, and the area of each slope class (in 10° intervals) was calculated. A landslide density (landslides/km^2 [LS/km^2]) was then calculated for each slope class. The slope angle at each landslide location (source area centroid) was also determined, and 25, 50, and 75 percentiles (Quartile 1 [Q1], median and Quartile 3 [Q3]) were calculated based on these landslide location slope angles for each geological unit and land-cover class (see below).

2 https://www.planet.com/

- **Rainfall:** Gauge-corrected rain radar data was provided by MetService. The 2021 54- and 2022 96-hour (storm totals) rain radar data were contoured into 50 mm contour intervals (isohyets), and the area covered by each interval was calculated. A landslide density (LS/km^2) was then calculated for each rainfall contour. The rainfall (storm total) values were extracted from the rain radar data for each landslide location, and Q1, median and Q3 values were calculated based on these landslide location rainfall totals for each geological unit and land-cover class (see below).
- **Geology:** The 1:250,000 regional geological map (after Heron [2020] – QMAP seamless data) was used to determine the geological materials of each landslide source area. QMAP data were clipped to the study area and the area of each geological unit calculated. A landslide density (LS/km^2) was then calculated for each geological unit.
- **Vegetation / land cover:** Vegetation and land-cover classes from LCDB v5, as mapped in 2018 at 1:50,000 scale (downloaded from https://lris.scinfo.org.nz/), were used to determine the land cover for landslide source areas. The 'Exotic Forest' and 'Forest – Harvested' categories were updated for this project (for both 2021 and 2022 storm events) using the Planet imagery mentioned above. We grouped broadleaved indigenous hardwood, fernland, gorse/broom, manuka/kanuka and matagouri / grey scrub into a 'Scrub' category, and low-producing grassland and high-producing exotic grassland into 'Pasture'. An 'Other' category (where <3% of landslides initiated) included gravel or rock, sand or gravel, tussock and sub-alpine shrubland in 2021 and gravel or rock, sand or gravel, landslide and built-up areas in 2022. LCDB5 data was clipped to the study area, and the area of each land-cover class was calculated. A landslide density (LS/km^2) was then calculated for each land-cover class.

Note that the total areas clipped to the study area are slightly different between QMAP and LCDB v5 because they were mapped at different scales: QMAP 1:250,000; LCDB v5: 1:50,000.

3.3 Landslide Distribution Assessment Results

Descriptions and photographs of the different types and severity of landslides triggered by the August 2022 storm, observed during the reconnaissance flight, are provided in Rosser et al. (in prep) and, for the July 2021 storm, Wolter et al. (2022). Based on these initial observations, most of the landslides triggered by the August 2022 event appeared to be shallow soil and debris slides and flows that mainly occurred in surface colluvium[3] and/or regolith[4]. Several larger, deeper-seated landslides were identified where old relict landslides had been re-activated (Figures 3.1 and 3.2). Clusters of shallow, smaller landslides also occurred within some of the relict ones.

From the desktop-based mapping using aerial and satellite photography, a total number of 3792 landslides were mapped for the 2021 event (Figure 3.3) and 3805 landslides for the 2022 event (Figure 3.4). The distribution of all 7597 landslides in relation to rainfall, geology and land cover are discussed in the next sections for each storm event separately.

3 Colluvium is any unconsolidated material, usually a range of fine sediments to rock blocks, that has moved downslope.

4 Regolith is any unconsolidated material, weathered *in situ* from bedrock.

Figure 3.1 Examples of landslides from the reconnaissance flight: (a) shallow soil and debris flows and (b) deeper-seated slide triggered on an existing relict landslide.

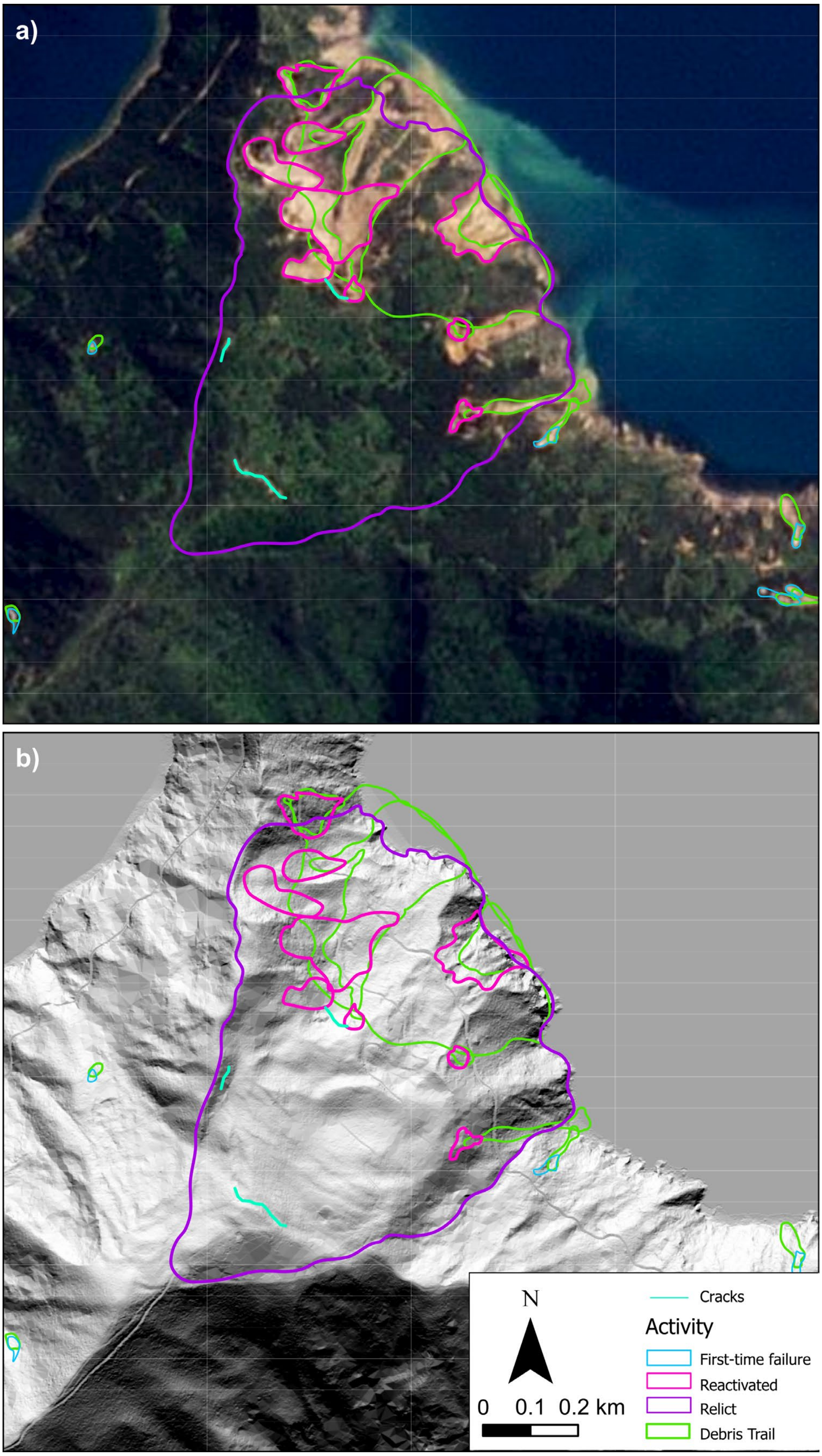

Figure 3.2 Example of a relict landslide on Forsyth Island that re-activated during the August 2022 storm event. (a) Post-storm Planet imagery showing mapped landslide polygons. (b) Landslide polygons from (a) overlaid onto the pre-event LiDAR. Note that the recent landslide debris polygons extend out into the sea compared to the pre-event imagery and LiDAR, indicating that debris has extended the coastline in some places. The area of the relict landslide is ~300,100 m^2, and the area of the re-activated landslides is about 110,000 m^2.

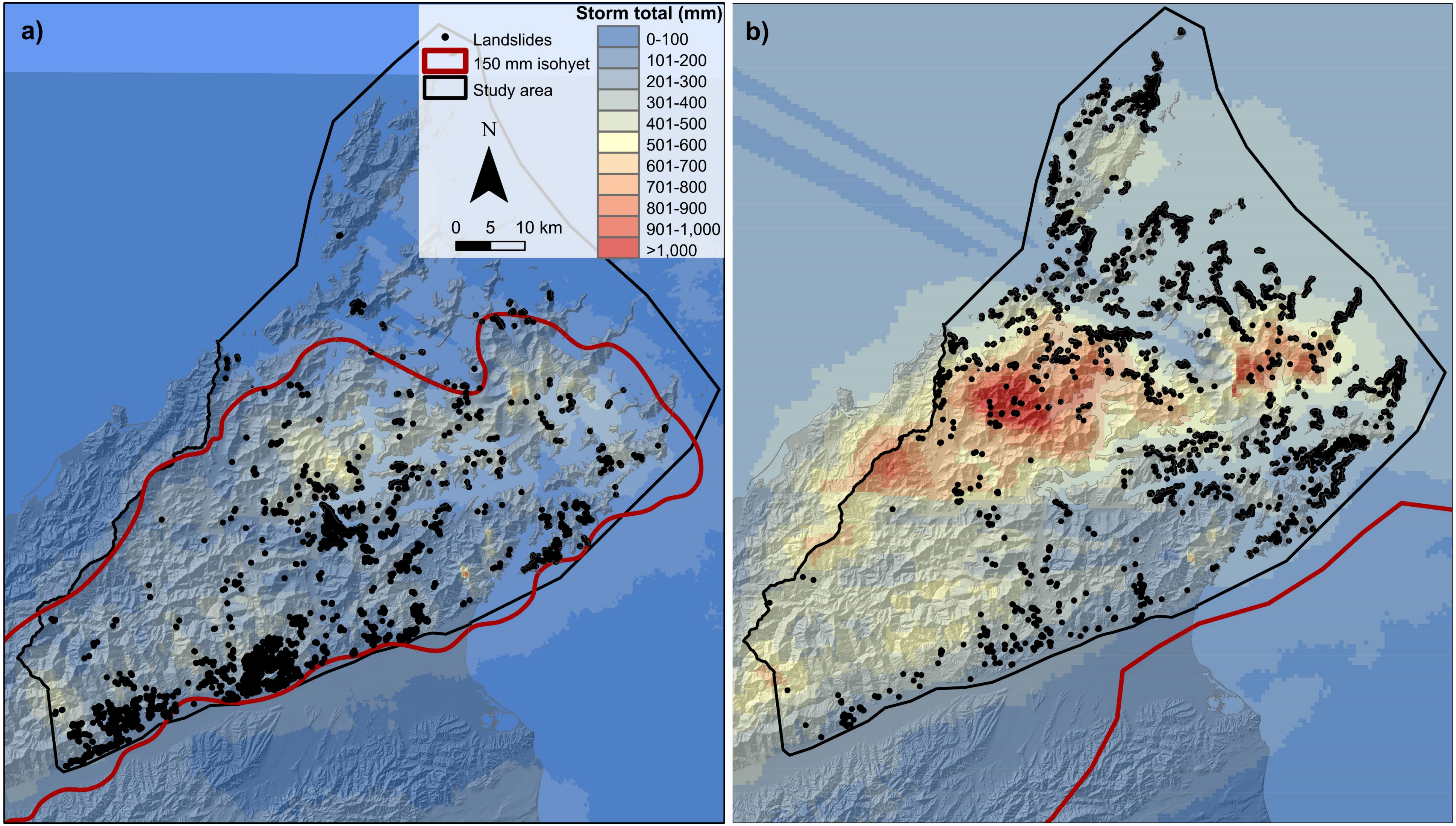

Figure 3.3 Landslide distribution and rainfall for the (a) July 2021 and (b) August 2022 storm events. Rainfall totals are listed as total storm amounts. Gauge-corrected rain radar was provided by MetService.

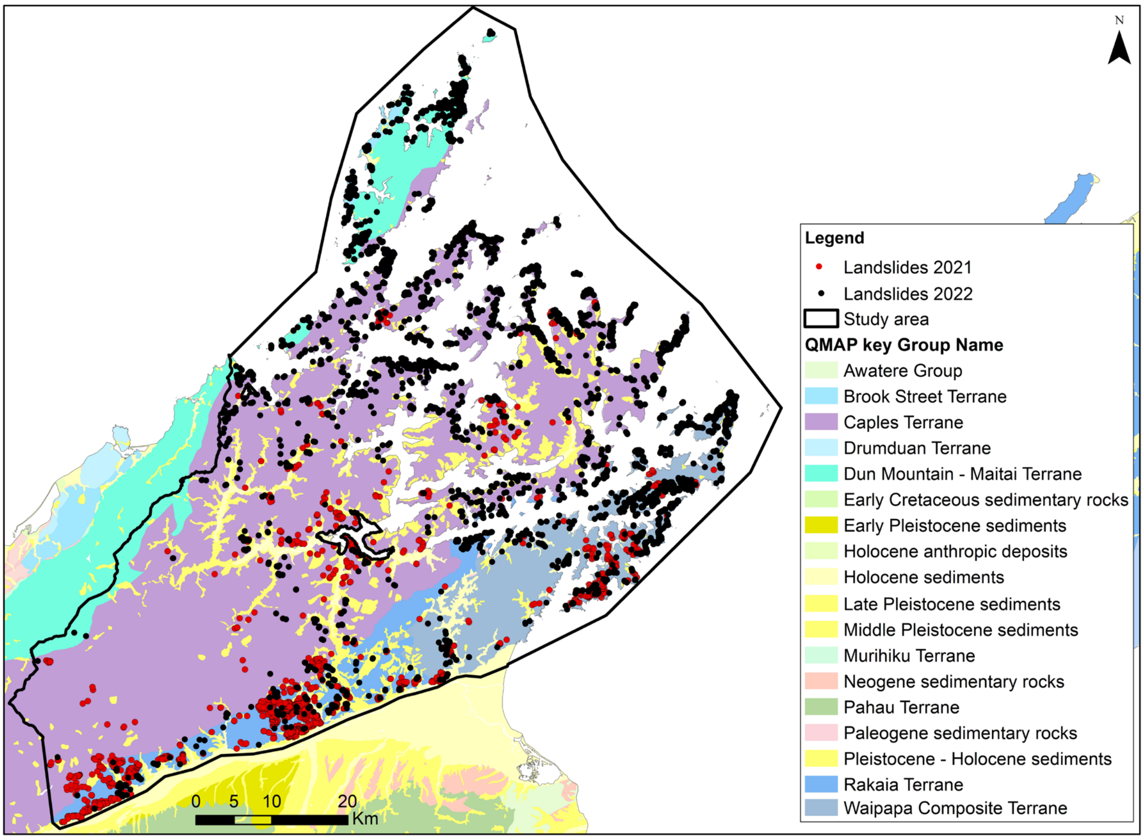

Figure 3.4 Locations of landslides triggered by the July 2021 (red) and August 2022 (black) storm events, shown in relation to the underlying geology from QMAP (Heron 2020).

3.3.1 2021 Storm

In the July 2021 storm, the greatest landslide density (2.5 LS/km^2) was in areas that received 200–250 mm of rain over the 54-hour storm. The highest landslide densities (>1.5 LS/km^2) were found in areas that received between 150 and 350 mm of rain (Table 3.1).

Table 3.1 Rainfall bands over the storm duration (54 hours) in which landslides occurred during the July 2021 storm, based on the area occupied by each rain band; percentage of total area occupied by each rainfall band; and landslide count, percentage and density. Rainfall was derived from MetService gauge-corrected rain radar data.

Rainfall (mm)	Area (km^2)	% Area	Landslide Count	% Landslide	LS/km^2
0–50	287.8	9.0	0	0.0	0
50–100	303.1	9.5	56	1.5	0.18
100–150	849.7	26.6	90	2.4	0.11
150–200	753.3	23.6	1507	39.8	2.00
200–250	513.3	16.1	1279	33.7	2.50
250–300	282.1	8.8	529	13.9	1.88
300–350	115.3	3.6	246	6.5	2.12
350–400	55.3	1.7	58	1.5	1.05
400–450	24.0	0.8	20	0.5	0.83
>450	12.2	0.4	7	0.2	0.57
Total	**3196.1**	**100**	**3792**	**100**	**1.12** [1]

[1] Average LS/km^2.

Almost half of the landslides (49%) occurred on slopes underlain by Rakaia Terrane pelitic schist (TZIIIB-IV) derived from sandstone/mudstone, despite this unit occupying <8% of the study area. This unit therefore was associated with the highest landslide densities (7.7 LS/km^2; Table 3.2) – nearly five times greater than the rock group with the next highest density (Waipapa Composite Terrane – 1.7 LS/km^2). Landslides occurred most frequently in highly metamorphosed Rakaia Terrane with 150–250 mm of rain and on slopes with angles between 30° and 50° (Figure 3.5). All geological units had similar median rainfall amounts at which landslides occurred (~200 mm), except for the Dun Mountain units (Figure 3.6a), which had a lower median rainfall value (and a smaller landslide count). All geological units had median slope angles at which landslides occurred between 30° and 40° (Figure 3.6b).

Table 3.2 QMAP (Heron 2020) key rock type group names in which landslides occurred during the 2021 storm, based on area occupied by different rock types; percentage of total area occupied by each rock type; and landslide count, percentage and density. Descriptions of QMAP key group names are listed in Appendix 4.

QMAP – Key Group Name	Area (km^2)	% Area	Rain Max. / Mean (mm)	Landslide Count	% Landslide	LS/km^2
Rakaia Terrane	238.4	7.8	323 / 205	1843	48.6	7.73
Waipapa Composite Terrane	351.2	11.4	971 / 207	603	15.9	1.72
Pleistocene–Holocene sediments [1]	249.3	8.1	660 / 241	289	7.6	1.16
Middle Pleistocene sediments	48	1.6	485 / 220	42	1.1	0.88
Late Pleistocene sediments	99.7	3.2	525 / 210	54	1.4	0.54
Caples Terrane	1825.9	59.4	674 / 234	926	24.4	0.51
Holocene sediments	151.5	4.9	178 / 163	30	0.8	0.20
Dun Mountain – Maitai Terrane	110.5	3.6	258 / 100	5	0.1	0.05
Total	**3174**	**100**	**971 / 197**	**3792**	**100**	**1.60 [2]**

[1] Including relict landslide deposits ranging from coherent rock masses to unsorted fragments in a fine-grained matrix.

[2] Average LS/km^2.

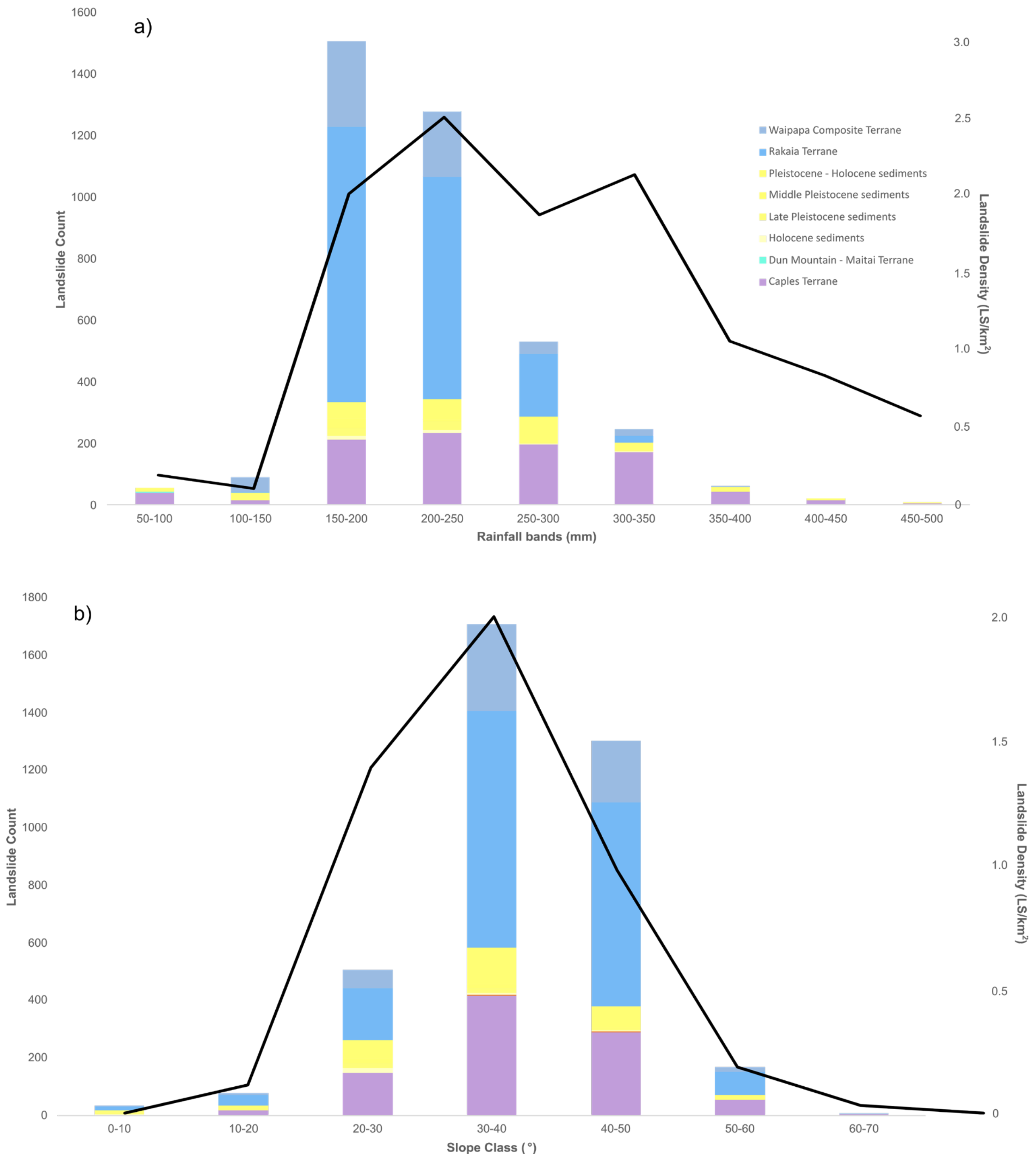

Figure 3.5 Landslide counts (bars) and densities (black curves) that occurred in QMAP key group names by (a) rainfall band (storm total) and (b) slope class during the 2021 event.

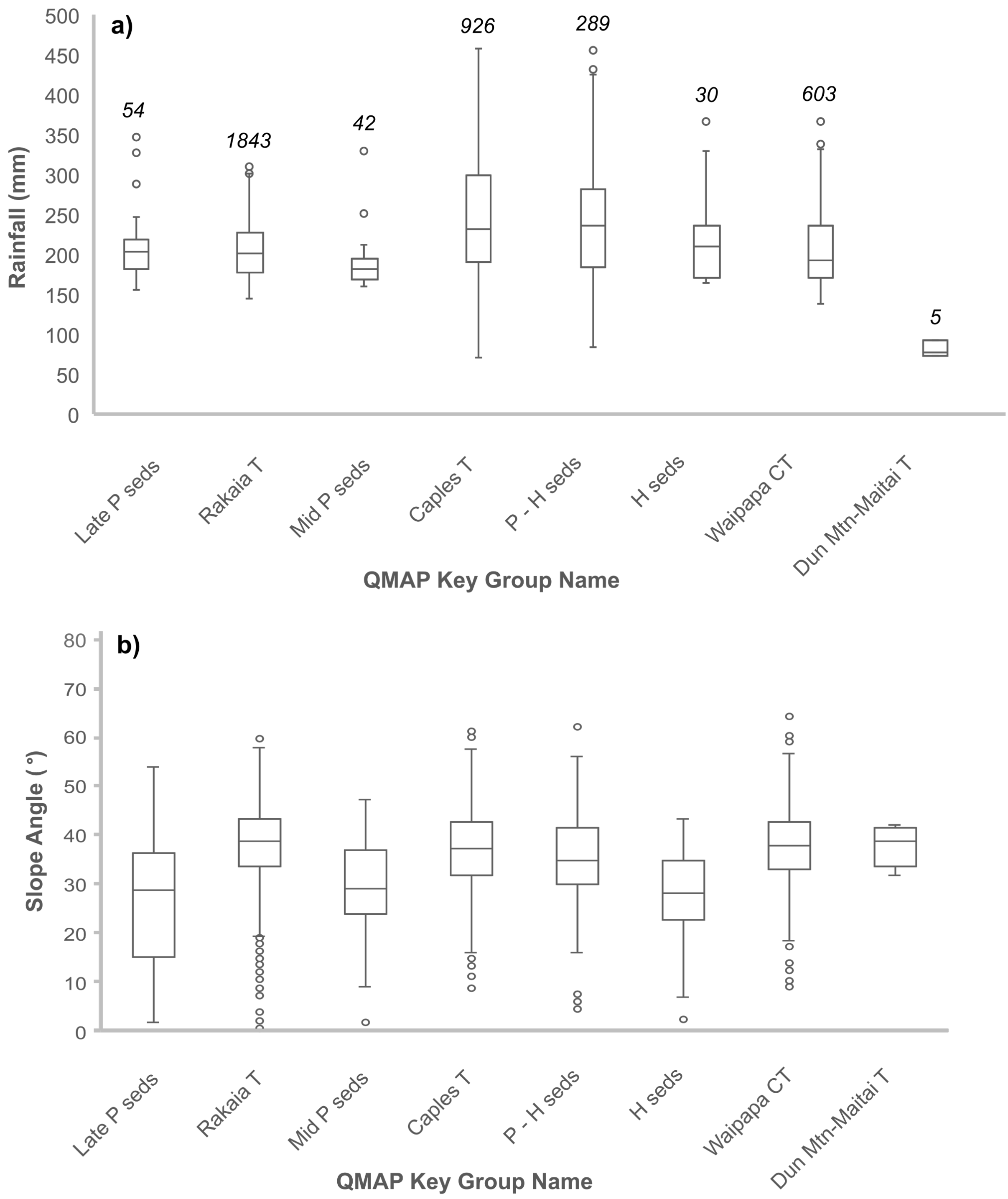

Figure 3.6 Box and whisker plots showing the (a) storm total rainfall and (b) slope angle at which landslides occurred in each of the main underlying geology types in 2021 at each mapped landslide location. Hollow circles represent outliers, which are defined as any value that is less than Q1 – (1.5 x IQR) or more than Q3 + (1.5 x IQR). Q1: first quartile (25%), Q3: third quartile (75%) and IQR: interquartile range (Q3–Q1). Italicised numbers indicate landslide count per group name.

The most common land-cover class that landslides initiated in was exotic (plantation) forest (35%), followed by harvested exotic forest (29%), scrub (19%) and pasture (12%) (Figure 3.7; Table 3.3). Areas of exotic or harvested forest where 150–250 mm rain fell had the highest landslide counts (Figure 3.8a), as did slopes between 30° and 50° in these land-cover classes (Figure 3.8b). Landslides most commonly initiated in exotic forest at slopes <60°.

Based on our analysis (see Section 3.2), landslides occurred in pasture with the lowest median and minimum (outlier) total storm rainfall (~150 mm and 70 mm, respectively; Figure 3.9a). Landslides occurred in planted and harvested exotic forest and scrub with median rainfalls of ~200–230 mm and in indigenous forest and 'other' land covers with the highest median values (>250 mm) (Figure 3.9a). Most land covers had Q1 rainfall totals of 75–80 mm, except harvested forest and 'other', which had Q1 values of >130 mm. Disregarding the outliers, the Q1 value represents the rainfall total above which 75% of the landslides occurred.

Median slope angles were between 34° (pasture) and 50° (other), with most land covers having median slope angles where landslides occurred between 38° and 41° (Figure 3.9b). The Q1 values above which 75% of values occurred varied by land cover, with the Q1 value for 'other' at 42° and pasture at 29°. Remaining land covers showed Q1 values between 32° and 34°, although landslides in indigenous forest occurred on slightly higher Q1 slope angles (36°). Outliers occurred on slopes <10° in all land-cover classes except 'other' (sand and gravel and gravel and rock – mostly steep coastal cliffs).

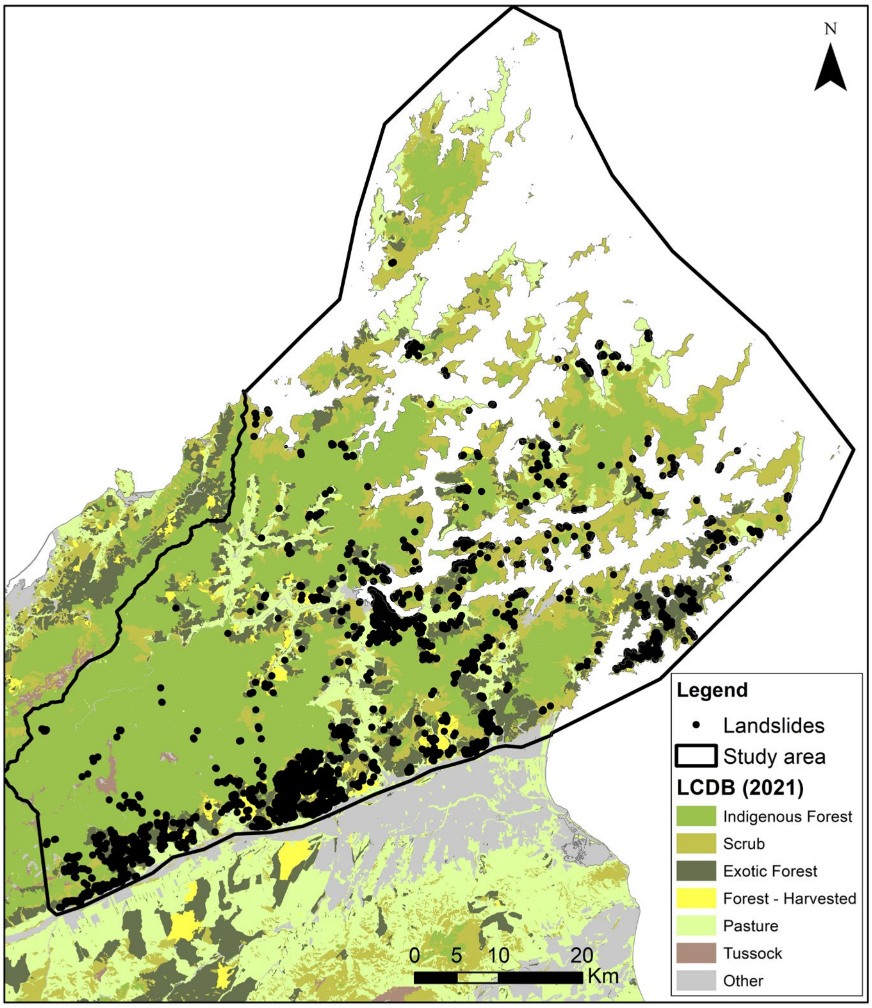

Figure 3.7 Locations of landslides (black points) that occurred during the July 2021 event, shown in relation to the land-cover classes from LCDB v5. The 'Forest' and 'Forest – Harvested' categories were updated using 2021 Planet imagery.

Table 3.3 LCDB v5 land-cover classes in which landslides occurred during the 2021 storm, based on area occupied by different land-cover classes; percentage of total area occupied by each land-cover class; and landslide count, percentage and density.

LCDB v5 Land-Cover Class	Area (km^2)	% Area	Rain Max. / Mean (mm)	Landslide Count	% Landslide	LS/km^2
Forest – Harvested	98.5	3.1	461 / 216	1090	28.7	11.07
Exotic Forest	437.9	13.7	534 / 213	1343	35.4	3.07
Pasture (Exotic grassland)	379.6	11.9	497 / 176	452	11.9	1.19
Scrub	757.5	23.7	541 / 194	727	19.2	0.96
Other [1]	79.8	2.5	444 / 179	13	0.3	0.16
Indigenous Forest	1438.8	45.1	971 / 239	167	4.4	0.12
Total	**3192.1**	**100**	**971 / 203**	**3792**	**100**	**2.76** [2]

[1] 'Other' includes gravel or rock, sand or gravel, tussock and sub-alpine shrubland.

[2] Average LS/km^2.

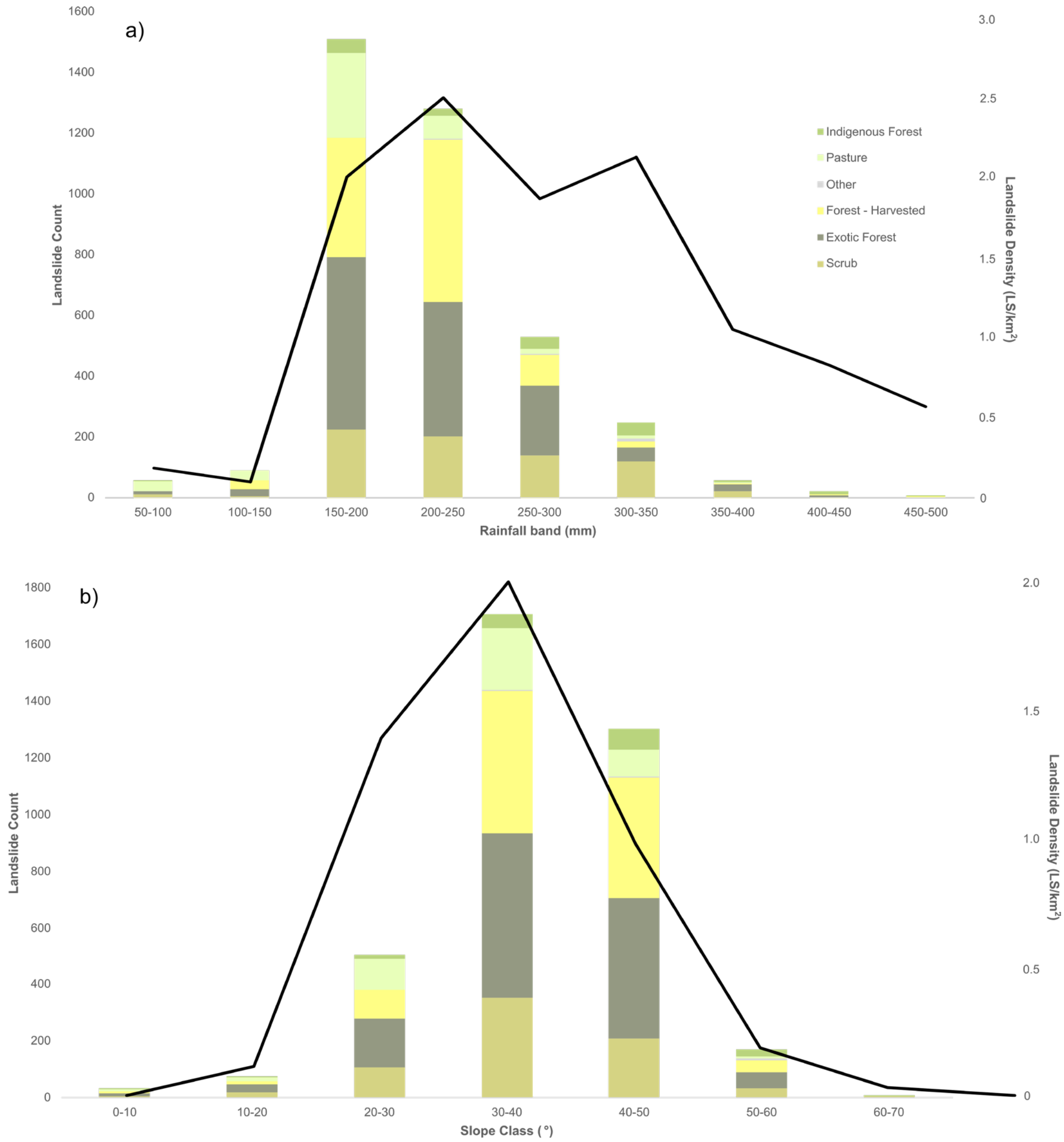

Figure 3.8 Landslide counts (bars) and densities (black curves) that occurred in LCDB v5 land-cover classes by (a) rainfall band (storm total) and (b) slope class.

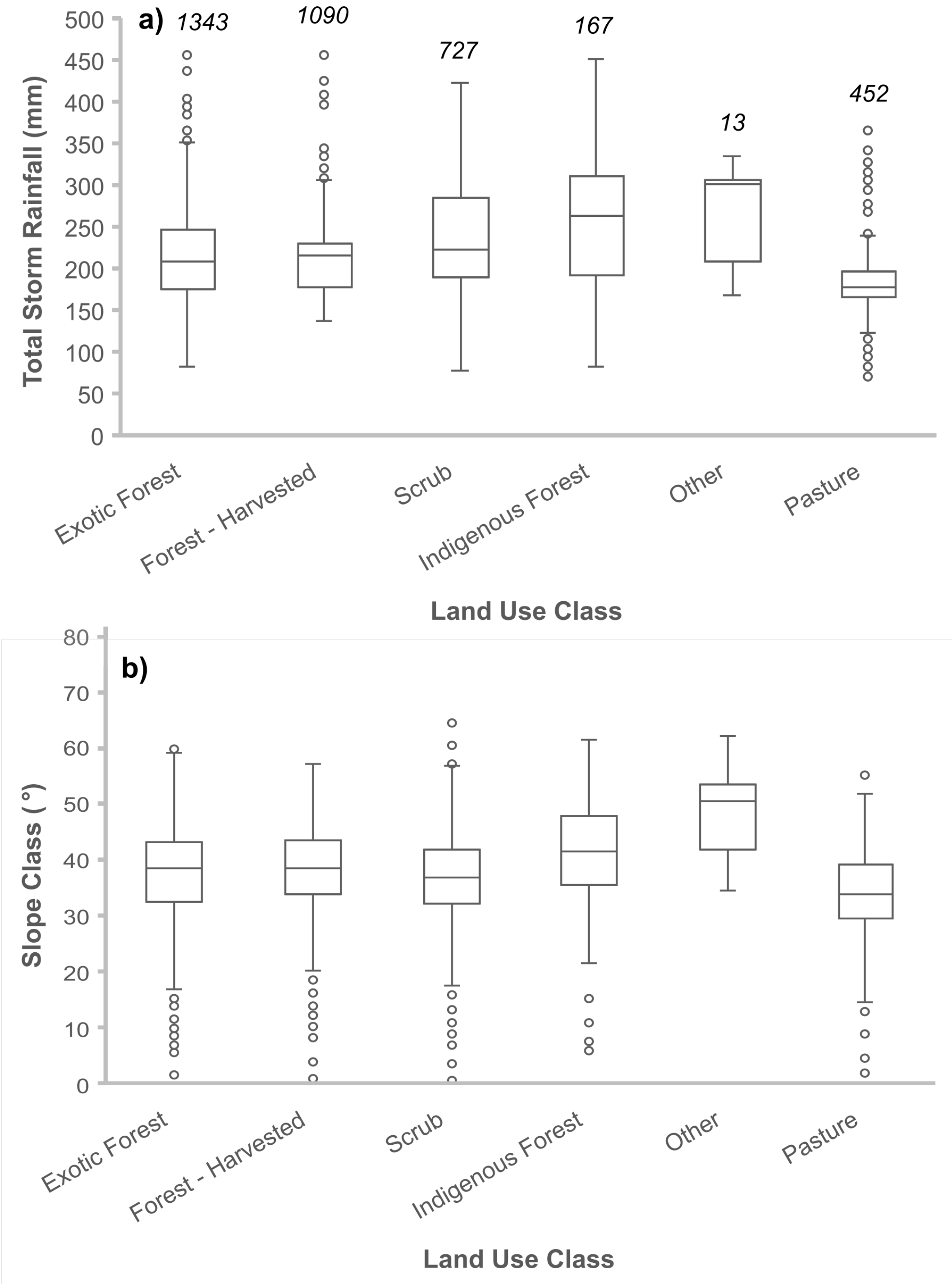

Figure 3.9 Box and whisker plots showing the (a) storm total rainfall and (b) slope angles at which landslides occurred in each of the main land-cover types during the 2021 storm. Hollow circles represent outliers. Italicised numbers indicate landslide count per land-cover class.

Summaries of the percent area covered by each of the storm total rainfall bands, slope angle classes, geological units and land-cover classes, as well as the landslides and landslide densities within each of these classes, are shown in Figure 3.10. From these plots, and Figures 3.5 and 3.8, proportionally more landslides (i.e. higher landslide densities) occurred in the 150–350 mm rainfall bands, on 20–50° slopes, within the Rakaia and Waipapa Composite terranes, and in exotic and harvested forest during the 2021 storm. Conversely, landslides in areas with rainfall totals below 150 mm and above 350 mm; slopes below 20° and above 60°; all geological units except the Rakaia and Waipapa terranes; and scrub (slightly), indigenous forest and other land-cover classes were all under-represented in the data.

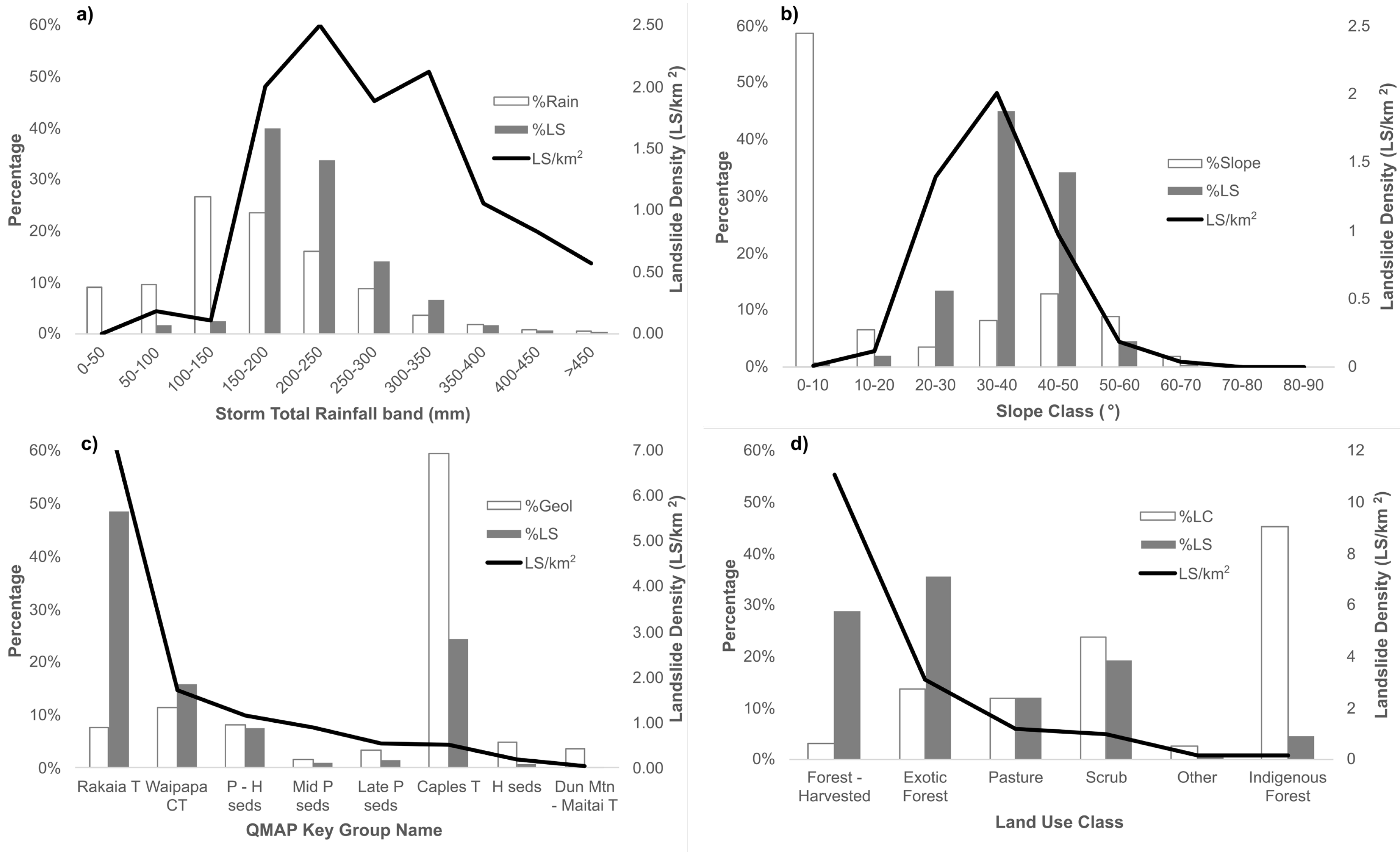

Figure 3.10 Percentages of the study area covered by each of (a) storm total rainfall, (b) slope angle, (c) geology (see Appendix 4 for definitions) and (d) land-cover classes (hollow bars) as well as the percentage of landslides within each of these classes (filled bars) and the landslide density per variable class (black lines, secondary axis) for the 2021 storm.

3.3.2 2022 Storm

In the August 2022 storm, the greatest landslide density (2.5 LS/km^2) occurred in areas that received 300–350 mm of rain over the 96-hour storm. Landslide densities >1.5 LS/km^2 occurred in areas that received between 250 and 400 mm of rain (Table 3.4).

Table 3.4 Rainfall bands over the whole storm duration (96 hours) in which landslides occurred during the 2022 storm, based on area occupied by different rainfall ranges, percentage of total area occupied by each rainfall band; and landslide count, percentage and density. Rainfall was derived from MetService gauge-corrected rain radar data.

Rainfall (mm)	Area (km^2)	% Area	Landslide Count	% Landslide	LS/km^2
0–150	0	0	0	0	0
150–200	13.2	0.4	2	0.1	0.15
200–250	182.1	5.6	163	4.3	0.89
250–300	432.3	13.2	637	16.7	1.47
300–350	443.7	13.6	1099	28.9	2.48
350–400	473.4	14.5	766	20.1	1.62
400–450	438.4	13.4	514	13.5	1.17
450–500	321.3	9.8	138	3.6	0.43
500–550	177.5	5.4	91	2.4	0.51
550–600	147.8	4.5	87	2.3	0.59
600–650	182.1	5.6	84	2.2	0.46
650–700	121.3	3.7	101	2.7	0.83
700–750	96.6	3.0	44	1.2	0.46
750–800	78.4	2.4	36	0.9	0.46
800–850	54.4	1.7	11	0.3	0.20
850–900	31.1	1.0	9	0.2	0.29
900–950	20.4	0.6	5	0.1	0.25
950–1000	7.5	0.2	0	0.0	0.00
>1000	46.2	1.4	18	0.5	0.39
Total	**3304.4**	**100**	**3805**	**100**	**0.70 [1]**

[1] Average LS/km^2.

In 2022, 38% of landslides occurred on slopes underlain by Caples Terrane semi-schist (TZIIA) bedrock and 25% on slopes underlain by Waipapa Composite Terrane semi-schist (TZIIA) (Figure 3.4; Table 3.5). Brook Street Terrane tuffaceous sandstone and siltstone had the highest landslide densities (6.8 LS/km^2) (Table 3.5; Figures 3.11 and 3.16). Most landslides occurred in the 300–350 mm rainfall band and 30–50° slope angle classes within the Caples Terrane unit (Figure 3.11).

The Holocene and Pleistocene–Holocene sediments, Caples Terrane and Dun Mountain – Maitai Terrane had Q1 values of 200–232 mm (Figure 3.12a), while other geological units had higher Q1 values up to 327 mm (Late Pleistocene sediments). All geological units had similar median rainfall where landslides occurred (280–400 mm), except for the Middle Pleistocene units (alluvial deposits and terrace gravels and only nine landslides), which had a higher median rainfall value of 608 mm (Figure 3.12a). Landslides occurred across the widest rainfall range (outliers excluded) in the Middle Pleistocene and Holocene sediments (floodplains and sand dunes). The Rakaia, Dun Mountain – Maitai (excluding outliers) and Brook Street terranes did not contain landslides that occurred in areas with >400 mm of rain over the storm duration. Only the Dun Mountain – Maitai Terrane received significantly more than 400 mm rain (Table 3.5).

Most geological units had median slope angles at which landslides occurred between 30° and 40° (Figures 3.11b and 3.12b): Murihiku Terrane and Holocene sediments had median values of ~25°, and Late Pleistocene units a significantly lower median of 8° (this unit only had three landslides within it and generally hosts slopes <10°).

Table 3.5 QMAP (Heron 2020) group names in which landslides occurred during the 2022 storm, based on area occupied by different rock types; percentage of total area occupied by each rock type; and landslide count, percentage and landslide density. Descriptions of QMAP key group names are listed in Appendix 4.

QMAP – Key Group Name	Area (km^2)	% Area	Rain Max. / Mean (mm)	Landslide Count	% Landslide	LS/km^2
Brook Street Terrane	16.3	0.5	331 / 308	111	2.9	6.81
Waipapa Composite Terrane	351.2	11.1	611 / 290	945	24.8	2.69
Pleistocene–Holocene sediments	249.3	7.9	1174 / 474	671	17.6	2.69
Dun Mountain – Maitai Terrane	191	6.0	898 / 447	381	10.0	1.99
Rakaia Terrane	238.4	7.5	462 / 307	217	5.7	0.91
Caples Terrane	1827.5	57.6	1270 / 512	1433	37.7	0.78
Holocene sediments	151.5	4.8	1063 / 351	35	0.9	0.23
Middle Pleistocene sediments	48	1.5	1023 / 470	9	0.2	0.19
Late Pleistocene sediments	99.7	3.1	1227 / 449	3	0.1	0.03
Total	**3172.9**	**100**	**1270 / 373**	**3805** [1]	**100**	**1.80** [2]

[1] Note that there was one landslide in Murihiku Terrane, included with Dun Mountain here.

[2] Average LS/km^2.

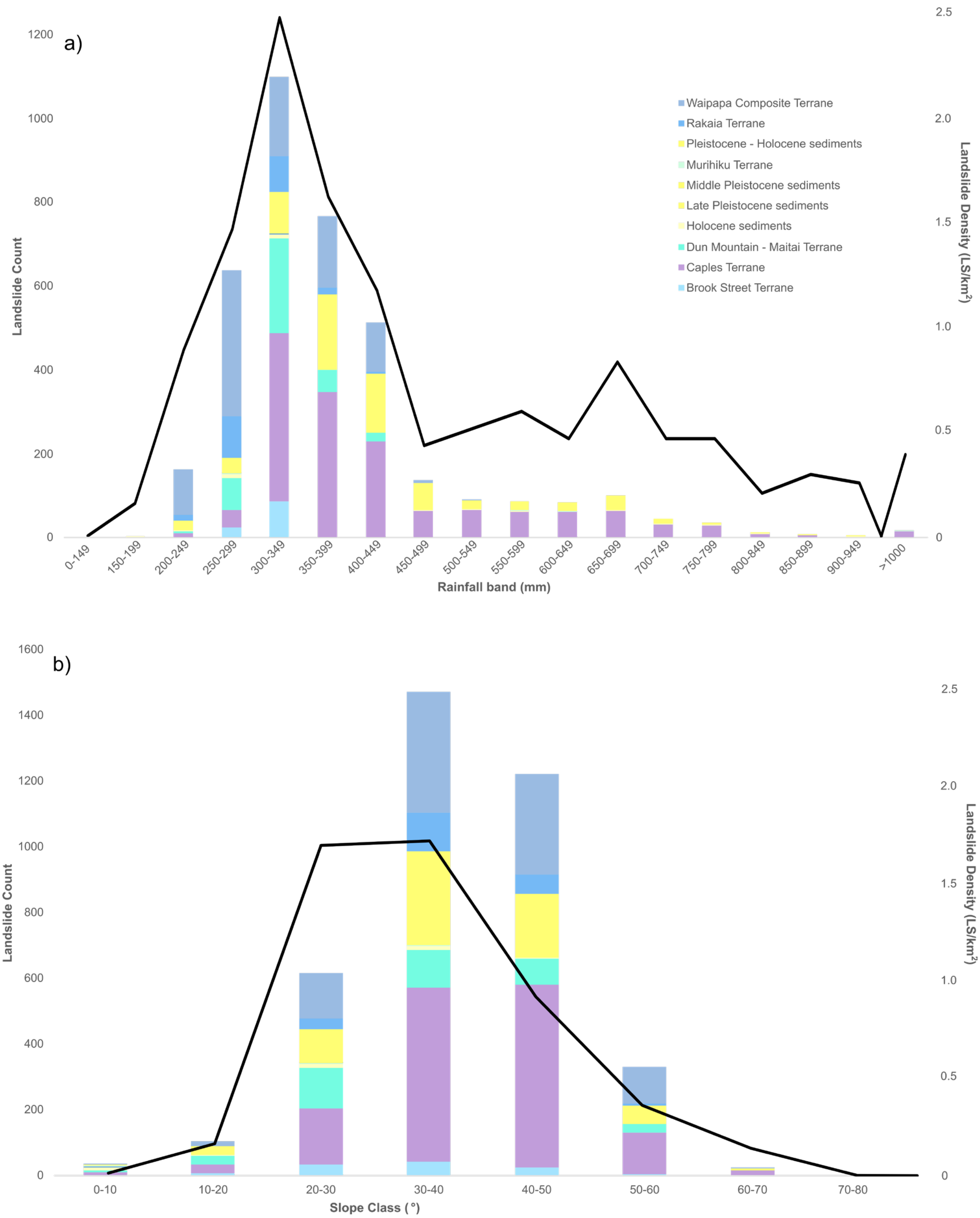

Figure 3.11 Landslide counts (bars) and densities (black curves) that occurred in QMAP key group names by (a) rainfall band (storm total) and (b) slope class in the 2022 event.

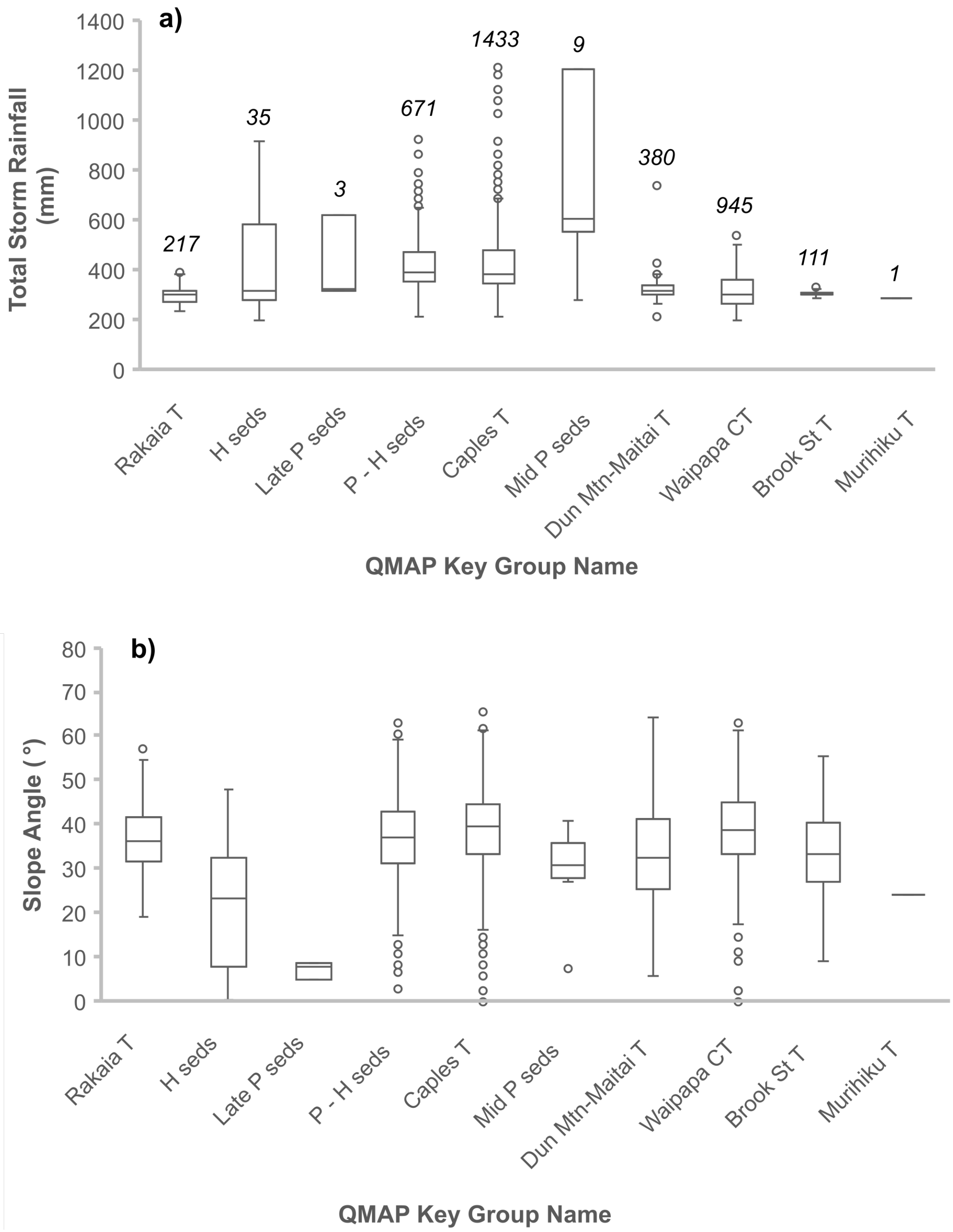

Figure 3.12 Box and whisker plots showing the (a) storm total rainfall (note different scale from 2021, Figure 3.6a) and (b) slope angle at which landslides occurred in each of the main underlying geology types. Hollow circles represent outliers.

Landslides that occurred during the 2022 storm are shown in relation to the LCDB v5 land-cover classes in Figure 3.13 and Table 3.6. Forty percent of landslides occurred in scrub and 37% in pasture (Table 3.6); the highest landslide densities were recorded in pasture. Exotic forest accounted for 9%, and both harvested forest and indigenous forest for 6% each, of landslides occurring during the August 2022 storm.

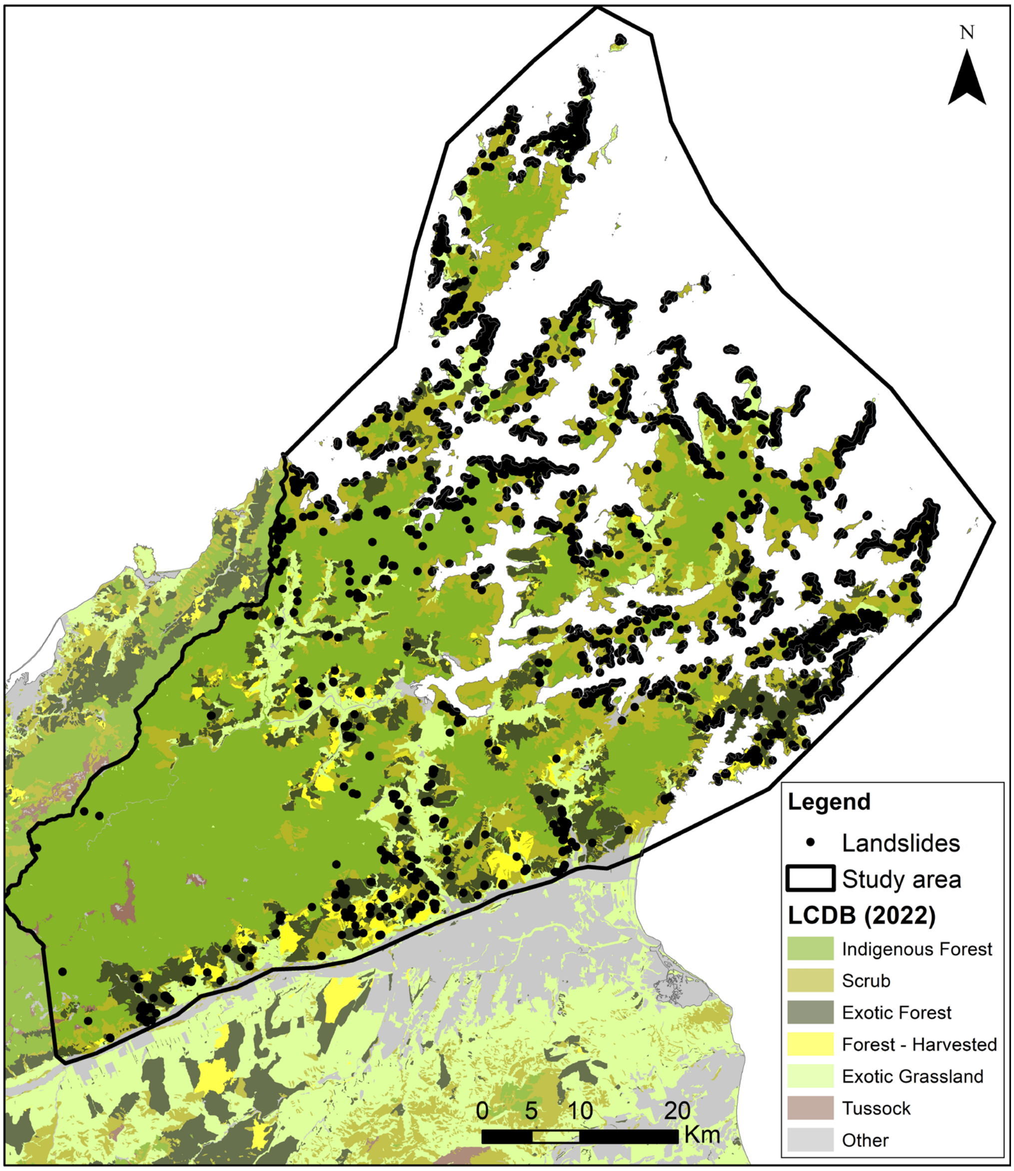

Figure 3.13 Locations of landslides (black points) that occurred during the July 2022 event, shown in relation to the land-cover classes from LCDB v5. 'Forest' and 'Forest – Harvested' categories were updated using 2022 Planet imagery. 'Exotic Grassland' = pasture.

Table 3.6 LCDB v5 land-cover classes in which landslides occurred during the 2022 storm, based on area occupied by different land cover classes; percentage of total area occupied by each land-cover class; landslide count, percentage and landslide density.

LCDB v5 Land-Cover Class	Area (km^2)	% Area	Rain Max. / Mean (mm)	Landslide Count	% Landslide	LS/km^2
Pasture	379.6	11.9	1227 / 389	1409	37.0	3.71
Scrub	756.4	23.7	1184 / 410	1530	40.2	2.02
Forest – Harvested	124.9	3.9	1200 / 377	224	5.9	1.79
Other [1]	79.8	2.5	1205 / 631	93	2.4	1.17
Exotic Forest	412.5	12.9	1115 / 381	338	8.9	0.82
Indigenous Forest	1438.8	45.1	1270 / 519	211	5.6	0.15
Total	**3192.1**	**100**	**1270 / 451**	**3805**	**100**	**1.61** [2]

[1] 'Other' includes built-up area, landslide, gravel or rock, and sand or gravel.

[2] Average LS/km^2.

Most landslides occurred in pasture and scrub at storm total rainfalls of 250–450 mm and at slope angles between 30° and 50° (Figure 3.14). Q1 values were consistently between 205 and 261 mm across land-cover classes for 2022 (Figure 3.15a), with pasture having the lowest Q1 value, followed by scrub, exotic forest, 'other' and harvested forest. Landslides occurred in indigenous forest with the highest Q1 value at 261 mm (and lowest landslide density, Table 3.6). Median total storm rainfalls for landslides were between 285 mm (harvested forest) and 370 mm (scrub), with an indigenous forest median value significantly higher at 686 mm. Pasture and 'other' land-cover classes did not contain landslides that occurred in areas with >914 and >492 mm of rain, respectively, during the storm (outliers included), even though they received >1100 mm of rain. All other land covers contained outliers that occurred in areas with >1200 mm of rain over the storm duration.

Median slope angles that landslides occurred on were remarkably consistent across land-cover classes – 36–39°, except 'other', where the median value was higher at 49° (Figure 3.15b). 'Other' included gravel and rock, sand and gravel (mainly steep coastal cliffs), landslide and built-up areas in 2022.

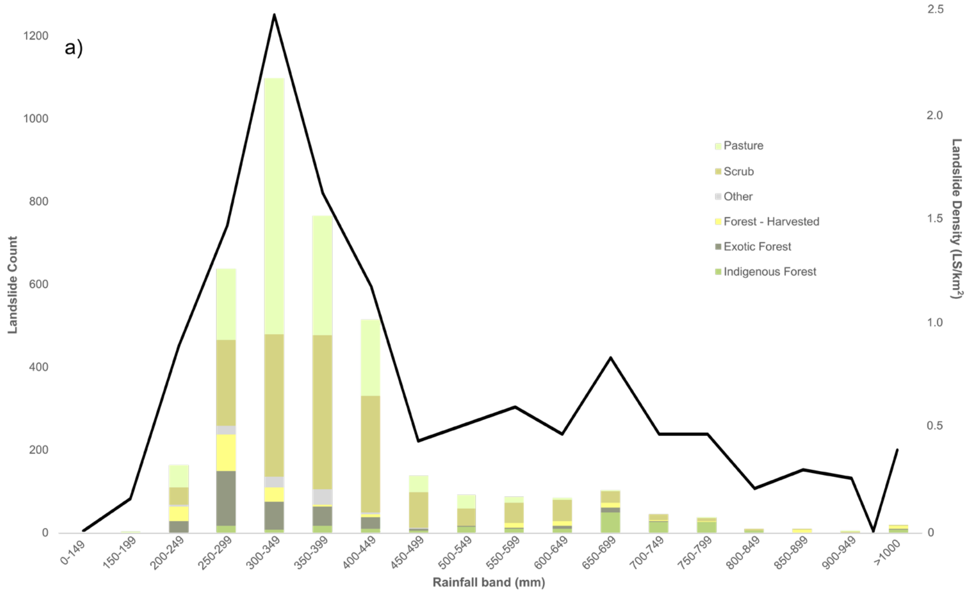

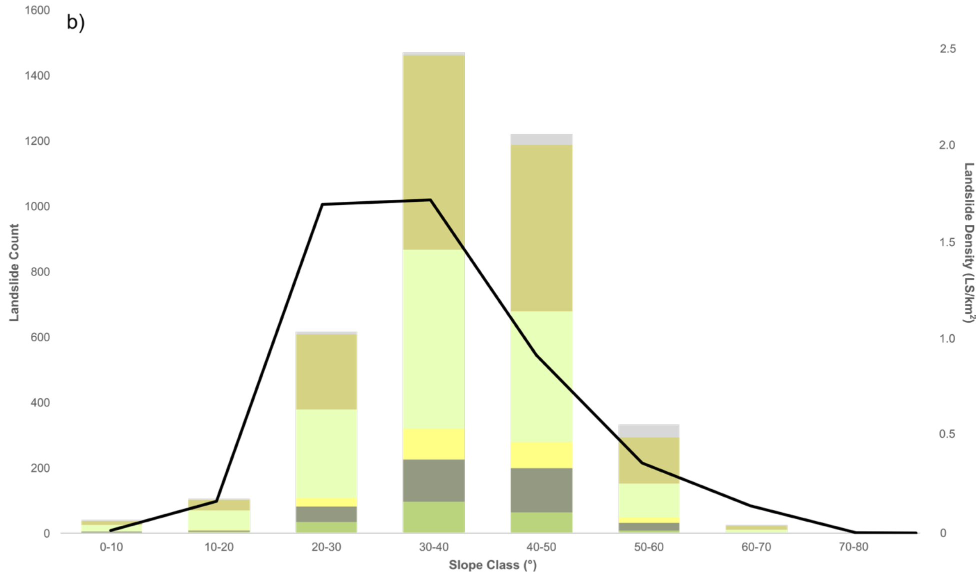

Figure 3.14 Landslide counts (bars) and densities (black curves) that occurred in LCDB v5 land-cover classes by (a) rainfall band (storm total) and (b) slope class in 2022.

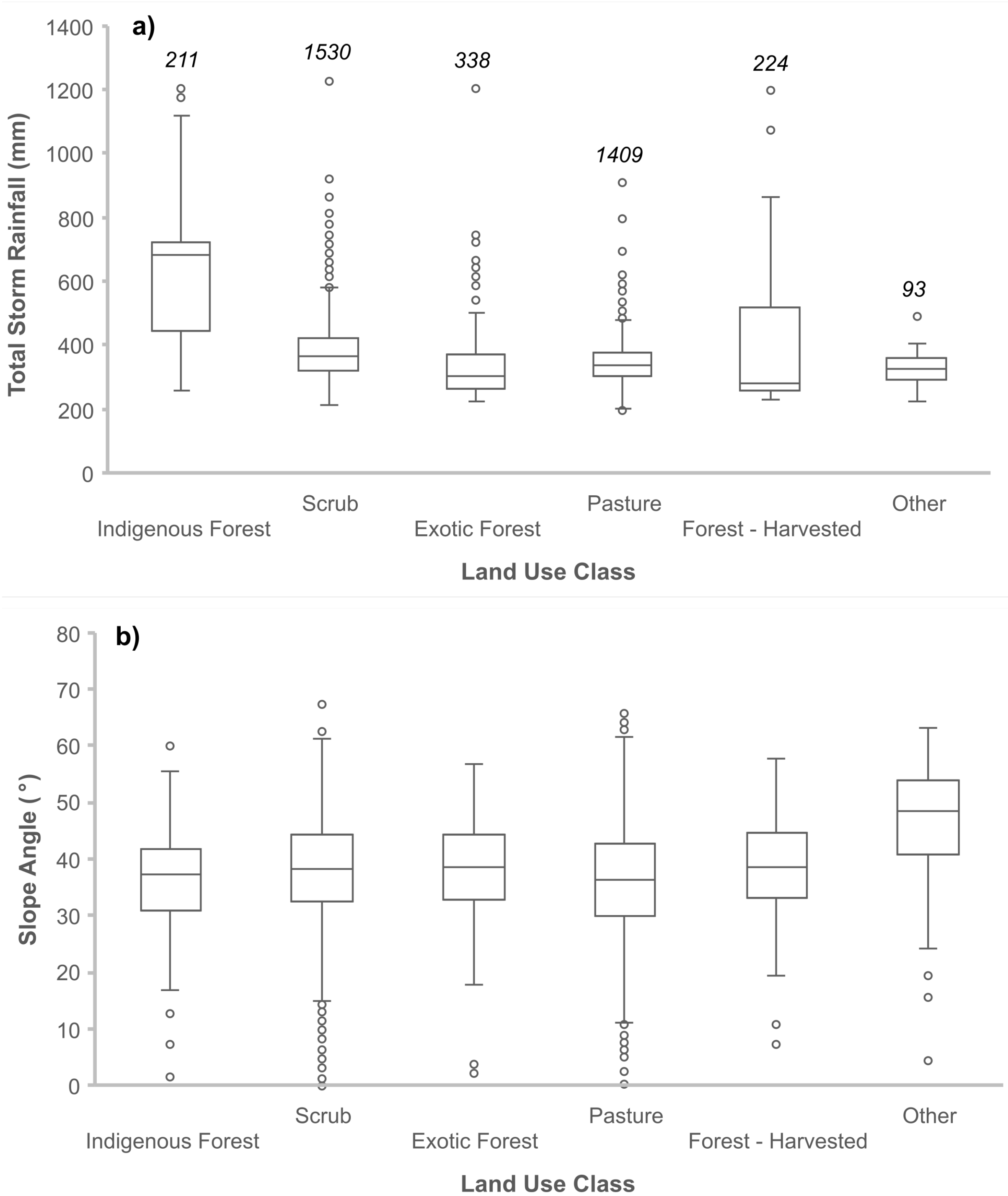

Figure 3.15 Box and whisker plots showing the (a) rainfall and (b) slope angles at which landslides occurred in each of the main land-cover classes in 2022.

Summaries of the percent area covered by each of the storm total rainfall bands, slope angle classes, geological units and land-cover classes, as well as the landslides and landslide densities within each of these classes, are shown in Figure 3.16. From these plots, and Figures 3.11 and 3.14, proportionally more landslides (i.e. higher landslide densities) occurred in 250–400 mm rainfall bands; on 20–50° slopes; within the Brook Street, Waipapa Composite and Dun Mountain – Maitai Terranes and Pleistocene to Holocene sediments; and in pasture, scrub,and harvested forest during the 2022 storm.

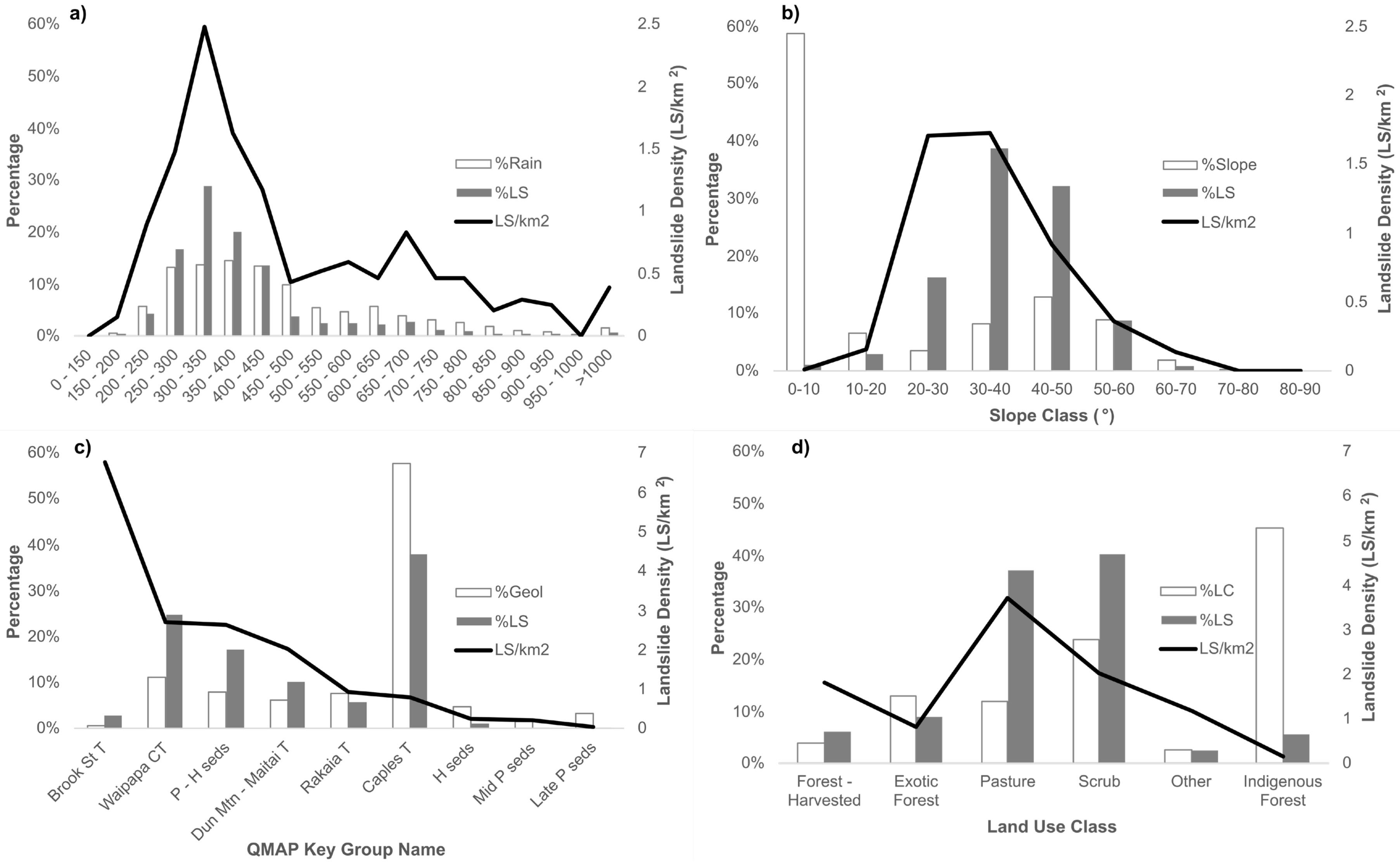

Figure 3.16 Percentages of the study area covered by each of (a) storm total rainfall, (b) slope angle, (c) geology (see Appendix 4 for definitions) and (d) land-cover classes (hollow bars), as well as the percentage of landslides within each of these classes (filled bars) and the landslide density per variable class (black lines, secondary axis) for the 2022 storm.

4.0 DETAILED CASE STUDY INVESTIGATIONS

4.1 Landslide Survey and Assessment Method

We used the same methods as for the 2021 storm, outlined in Wolter et al. (2022), to complete detailed investigations of selected case study landslides that impacted dwellings during the August 2022 storm. These methods included:

1. Surveying each site with a DJI Phantom 4 Advanced 2 Remotely Piloted Aerial System (RPAS) to obtain high-resolution DSMs of each site.
2. Making observations on landslide source and debris trail characteristics, surveying damage heights along building walls and mapping each landslide.
3. Assessing the structural and non-structural damage to each dwelling impacted by a given landslide. Impact included both debris inundation, where landslide debris travelling downslope impacted buildings, and slippage, where dwellings were under-mined by the landslide source area (see also Massey et al. [2019]).

Nine sites (Figure 4.1) were selected in consultation with MDC using the following criteria:

- Landslide type (representative landslide types observed during the 2022 storm were selected).
- Building damage (representative spectrum of building damage due to landslides was selected).
- Insurance (properties that were insured were preferentially selected, as this facilitates the development of fragility functions).
- Logistics (site access and time constraints).

Some general observations about road damage from landslides were also recorded and photographs were taken. The survey team was based in Blenheim during the detailed investigations, and data collection was limited by road closures and travel delays due to damage along roads, highlighting the impact of the storm on the road infrastructure. One day was spent on inspecting sites that had no road access. Access was gained by sea using a MDC Harbours vessel. The vessel was in high demand as part of the storm response, so we were not able to visit sea-access-only properties in the Pelorus Sound.

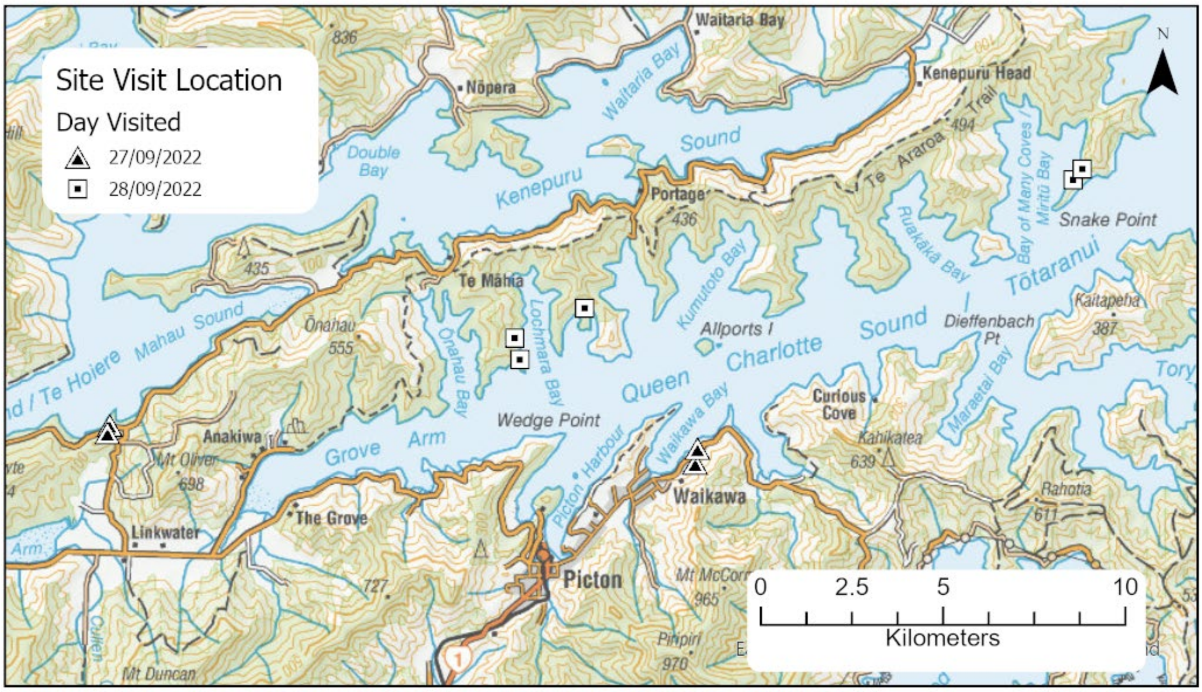

Figure 4.1 Location of landslides triggered by the August 2022 storm selected for detailed site investigations.

4.1.1 RPAS Surveying and Analysis Methods

Remotely Piloted Aircraft Systems (RPAS), commonly referred to as drones, are an effective tool for mapping the impacts of landslides (Lucieer et al. 2013). We used Structure from Motion (SfM) to reconstruct the landslides in 3D. Ground Control Points (GCPs) were used to accurately position the SfM models spatially, which allowed us to make a volumetric assessment of surveyed landslides.

The RPAS used was a DJI Phantom 4 Advanced 2. Flight paths were planned and executed using an application called Drone Harmony, which enabled the RPAS to fly a terrain following a double grid pattern. Flight altitudes were typically conducted at 40–50 m above the ground / top of present vegetation, based on pre-event LiDAR. Photos were collected with a gimble angle of -80°, a side overlap of 70% and a forward overlap of 60%. The GCPs used were five Propeller AeroPoints, which were placed on the ground in areas of unobscured sky coverage and passively collected centimetre-accurate GPS positions. The photos were then processed in Agisoft Metashape to generate DSMs, orthomosaics and 3D models of each landslide, with resolutions typically between 2 and 4 cm/pixel for the DSMs and 1 and 2 cm/pixel for orthomosaics. The outputs were used to map the source and debris trail polygons of each landslide for each of the nine detailed case studies (Figure 4.2).

Figure 4.2 Example of landslide mapping based on RPAS imagery.

To calculate the volume of each landslide, DSMs were generated at 1 m x 1 m cell size to match the resolution of the pre-event LiDAR data (MDC LiDAR 1 m DEM [2020–2021]). Vegetation overhanging, and therefore obscuring, any landslide was removed from the RPAS DSM where possible via automatic point cloud classification in Agisoft Metashape to better match the RPAS data to the LiDAR DEM. The depths of erosion and deposition were obtained using the Raster Calculator in ArcPro to subtract the pre-event LiDAR ground surface from the post-event RPAS ground surface. These values within the source and debris trail areas were classified into positive (deposition) and negative (erosion) change and then summed together to produce volumes for the landslides in m^3 (Appendix 1).

Maps of the orthomosaics, DSMs, change models (areas of erosion and deposition) and links to the 3D models are in Appendix 2.

4.1.2 Landslide Observations: Results

Of the nine landslides that impacted dwellings that we visited for more detailed field investigations, six were complex landslides, usually debris slump-slides (Figure 4.3; Table 4.1). Source volumes, based on the mapped source polygons and method described in Section 4.1, ranged from 58 m^3 to ~4000 m^3 and debris trail volumes from 23 m^3 (where debris had been cleared away) to ~9200 m^3 (Table A1.1). Note that these are conservative values due to uncertainties caused by overhanging vegetation. Landslide deposit volumes ranged from 1 to 2.4 times the source volumes, indicating entrainment and bulking (including large woody debris) as landslides moved downslope. Four landslides noticeably scoured the slopes in the debris path, with scour volumes up to 1800 m^3. In several cases, the calculated deposit volume was less than source volume due to:

1. Clearing and manual removal of material before the surveys.
2. Deposit entering water (we cannot quantify the underwater volume with photogrammetric surveys alone).
3. Post-landslide scour in the deposit area.

Figure 4.3 Examples of landslides visited during field investigations. (a) A debris spread/flow that impacted the back of a home; debris had been cleared by the time we visited (landslide ID 22-1). (b) The debris trail of a debris flow/flood, looking up towards the source and showing woody debris and the landslide material (22-2). (c) An example of slippage undermining a house (22-3). (d) Ground cracking at the source of a debris slump/slide (22-6). (e) Source area looking down the debris trail of a debris slump/flow (22-8). (f) Debris avalanche on very steep slope (22-9).

Source material was usually colluvium, with greywacke and schist bedrock at variable depth. Two landslides contained artificial fill to depths of 50–60 cm, and the maximum clast[5] length in the colluvium was 7–40 cm.

5 Here, 'clast' refers to cohesive rock blocks, not landslide debris blocks or agglomerate.

Table 4.1 Summary of landslide sites visited during the field assessments. See Tables 4.3 and 4.5 for building damage details.

Landslide ID	Landslide Type	Buildings Surveyed	Impact Type
22-1	Debris spread/flow	1	Debris inundation
22-2	Debris flow/flood	1	Debris inundation
22-3	Retrogressive slump	1	Slippage
22-4	Rotational slide	1	Debris inundation
22-5	Debris flow	1	Debris inundation
22-6	Debris slump/slide	1	Slippage
22-7	Debris slump/flow	1	Debris inundation
22-8	Debris avalanche	1	Debris inundation
22-9	Debris slump/slide	1	Slippage

Ground cracking at and above landslide headscarps indicated incipient and ongoing slope instability – more material could mobilise in future. Ground cracks were a maximum of 10 m long and open a maximum of 0.5 m wide. See Figure 4.4 for an example of ground crack (surface deformation) mapping.

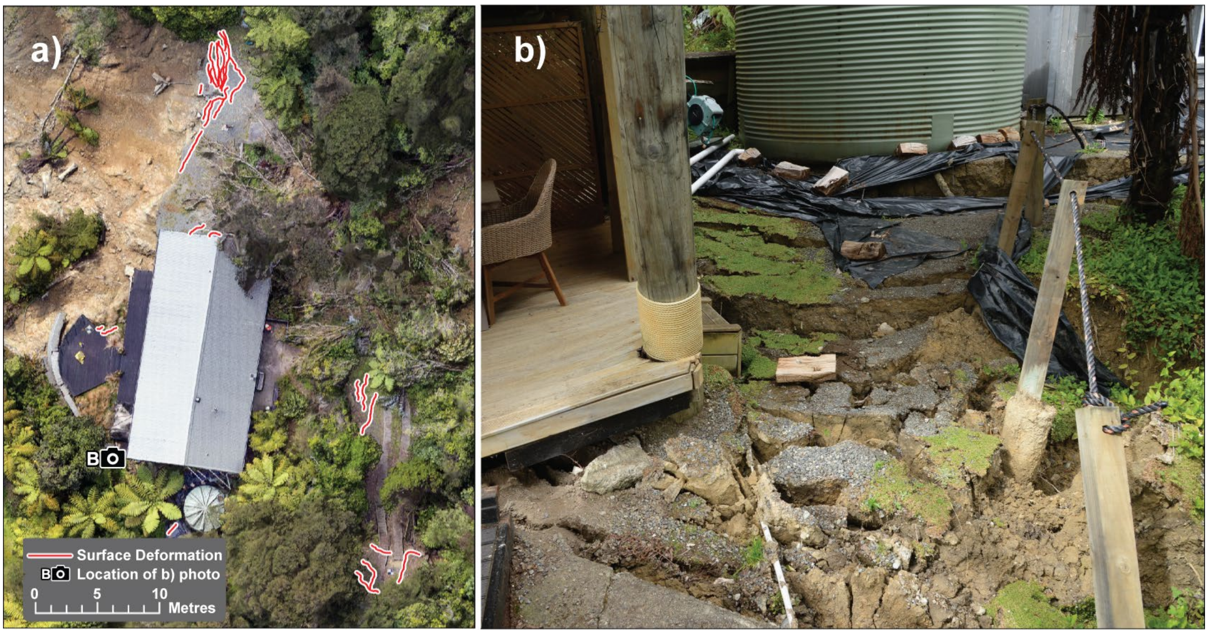

Figure 4.4 Example of surface deformation (cracking) at LS 22-3. (a) Location of cracks mapped from orthomosaic photos. (b) Extensive cracking obscured from the orthomosaic by vegetation.

4.2 Buildings Impacted

4.2.1 Building Assessment Methodology

As in 2021 (Wolter et al. 2022), each surveyed building's structural and non-structural attributes and damage were visually inspected from either the street adjacent to the affected building or from the building site (e.g. Figure 4.5). All information collected was recorded via survey forms with pre-populated fields related to building attributes and damage (Appendix 3.1). A unique anonymous identifier was assigned to each building. Photographs were taken to record building characteristics and observed damage.

Figure 4.5 Inspecting and assessing structural damage to a boatshed impacted by a debris flow.

For structural building damage, the level of damage sustained is expressed in terms of an ordinal categorical variable, whereby damage states represent all possible outcomes. This means that damage represented in each state must increase relative to increasing hazard intensity, i.e. 'no damage' to 'complete damage'. This approach is commonly employed in building damage assessments for earthquake and tsunami hazards to support the subsequent development of fragility functions. The structural building damage-state criteria developed for the Marlborough landslide survey is presented in Table 4.2. This criterion was informed from previous landslide damage surveys conducted in Marlborough for the July 2021 storm (Wolter et al. 2022), Wellington (Cyclone Dovi 2022) and Napier (November 2020) (reports pending), as well as lessons from the Canterbury earthquake sequence (Massey et al. 2014, 2019).

Non-structural damage in this survey relates to building contents, stock and equipment. Non-structural building components were included in the structural building damage-state criteria (Table 4.2). The difficulty of deriving precise estimates of the proportion of damage sustained by non-structural building items relative to their replacement cost (i.e. 'cost of repair' / 'cost of replacement') during field surveys means that an ordinal criteria of damage ratio bands was also developed. Where possible, surveyors inferred damage ratios based on damaged items left *in situ* at the building site or building damage observed.

Residential building habitability was recorded for each building at the time of visit. Residential buildings were deemed either habitable or uninhabitable based on their damage. Building safety inspection by MDC (i.e. colour tag, such as yellow [restricted access] or red [entry prohibited]) was also recorded if available.

Table 4.2 Building damage-state classification used in the Marlborough building survey.

Damage State	Damage Classification	Description of the Observed Damage	Damage Ratio
DS0	**None:** No damage	Damage is outside building footprint	0
DS1	**Insignificant:** Minor non-structural damage	Superficial (non-structural) inundation or <10% of building footprint is undercut	0–0.2
DS2	**Light:** Non-structural damage only	Superficial (non-structural) inundation or <10% of building footprint is undercut	0.2–0.4
DS3	**Moderate:** Reparable structural damage	Structural damage, or house is displaced	0.4–0.6
DS4	**Severe:** Irreparable structural damage	Structural damage, or house is displaced	0.6–0.8
DS5	**Critical:** Structural integrity fails	Impact-induced collapse, or >50% of building is undercut	0.8–1.0

4.2.2 Observations of Buildings Impacted: Results

Over the two-day survey period, nine landslide-affected buildings were visited. Four out of nine were in urban or rural residential areas (e.g. Waikawa and Moetapu Bay), while the rest were isolated buildings located in the Marlborough Sounds. For each building, structural and non-structural attributes were surveyed, damage was assessed and categorised, and general observations of the building and damage were recorded. This section summaries the data and observations collected from the landslide-affected buildings. The original observed dataset is also available in Appendix 3.2.

4.2.2.1 Building Attributes

As the survey objective was to collect empirical information on landslide damage to New Zealand buildings for the purpose of developing landslide vulnerability models, a broad range of building types were visited. A summary of the structural attributes recorded is presented in Table 4.3, with brief descriptions in this section:

1. **Building use:** Residential buildings were the only building use surveyed.
2. **Building age:** Ages of the surveyed buildings were evenly distributed among three house-design vintages; namely, pre-1960, 1960–1979 and post-1980.
3. **Foundation type:** Timber piles without brace foundations were used for the majority of the buildings surveyed, followed by concrete slab and concrete/steel pile foundations.
4. **Construction type and materials:** Timber frame is the only construction type for all of the surveyed buildings, which was expected given their residential use. The high proportion of weatherboard sheet-metal claddings for external walls and roofs were also expected for typical houses in New Zealand.
5. **Roof frame and slope:** Roofs constructed of timber material and of a mild slope (11–30°) were common in all surveyed buildings.
6. **Storeys:** The majority of the buildings surveyed were two-storey houses.

Table 4.3 Summary of building attributes for landslide-affected buildings surveyed in the Marlborough region after the 2022 storm.

Building Attributes		Count
Age	Pre-1960	3
	1960 –1979	3
	Post-1980	3
Foundation	Concrete slab	2
	Concrete rim/perimeter	1
	Rib-raft	0
	Timber pile without brace	5
	Timber pile with brace	1
	Concrete/steel pile	0
Construction type	Timber	9
	Brick masonry	0
	Concrete masonry	0
	Tilt-up panel	0
	Advanced design	0
Wall cladding	Weatherboard	8
	Stucco/roughcast	1
	Brick veneer	0
	Stone	0
	Fibre cement plank	0
	Fibre cement sheet	0
	Concrete masonry	0
	Sheet metal	0
	Corrugated iron	0
Roof frame	Timber	9
	Steel	0
	Concrete slab	0
Roof slope	Steep (>30°)	0
	Mild (11–30°)	7
	Near-flat (1–10°)	2
	Flat (0°)	0
Roof cladding	Sheet metal	9
	Clay/concrete tile	0
	Metal tile	0
	Slate	0
	Asphalt and fibreglass singles	0
	Sheet membranes on plywood sheet	0
	Concrete	0
	Timber	0
Storey	1	3
	2	6
	3 or more	0

4.2.2.2 *Building-Impact Data Results*

1. **Landslide type:** Most of the surveyed buildings (five) were affected by debris slumps/ slides. One building was affected by debris avalanches, while three were affected by debris flows/floods. Six buildings were inundated, and three were affected by slippage.
2. **Estimated tag:** To protect human safety, inspection by MDC or emergency response personnel resulted in a building being tagged: White (W), Yellow (Y1 and Y2) or Red (R1 and R2) (Table 4.4; Building Performance [2023]).
3. **Habitability:** Building habitability was recorded at the time of the detailed surveys. As the surveys were conducted days after the event, it is highly likely that many damaged buildings initially identified as habitable by MDC were not inhabited immediately following the event and so have been labelled as 'unoccupied'.
4. **Estimated damage state:** The damage-state criteria presented in the previous section were applied to estimate damage-state values for all buildings surveyed. At each location, accessible damaged and non-damaged buildings were surveyed within the time available. One of the assessed buildings sustained no damage (DS0), one DS2 and one DS3. Three buildings each were assigned to DS1 and DS5. Selected photographs of surveyed buildings in various damage states are available in Appendix 3.2.

Table 4.4 Definition of different building colour-tagging categories assigned by Marlborough District Council.

Tag	W	Y1	Y2	R1	R2
Definition	Can be used	Restricted access to part(s) of the property only	Restricted access – short-term entry only	Entry prohibited (at risk from external factors)	Entry prohibited (severe damage to building)

Table 4.5 Summary of building impact for buildings surveyed in the Marlborough region 2022.

Building Attributes		**Count**
Landslide type	Debris flow/flood	2
	Debris slump/slide/spread	**6**
	Debris avalanche	**1**
Impact type	Debris inundation	6
	Slippage	3
Estimated placard	None	2
	W	0
	Y1	2
	Y2	1
	R1	1
	R2	3
Habitability	Unhabitable	4
	Habitable (Occupied)	1
	Habitable (Unoccupied)	4
Estimated damage	DS0 (0); None: No damage	1
	DS1 (0–0.2); Insignificant: Minor non-structural damage	3
	DS2 (0.2–0.4); Light: Non-structural damage only	1
	DS3 (0.4–0.6); Moderate: Reparable structural damage	1
	DS4 (0.6–0.8); Severe: Irreparable structural damage	0
	DS5 (0.8–1.0); Critical: Structural integrity fails	3

The damage ratio of buildings in the Marlborough region compared to maximum debris heights of landslides for the July 2021 and August 2022 storms are shown in Figure 4.6. Compared with earthquake-triggered landslides (Massey et al. 2019), damage ratios appear to be lower for rainfall-triggered landslide impacts. Note that this work is currently being refined as part of an ongoing research project at GNS Science.

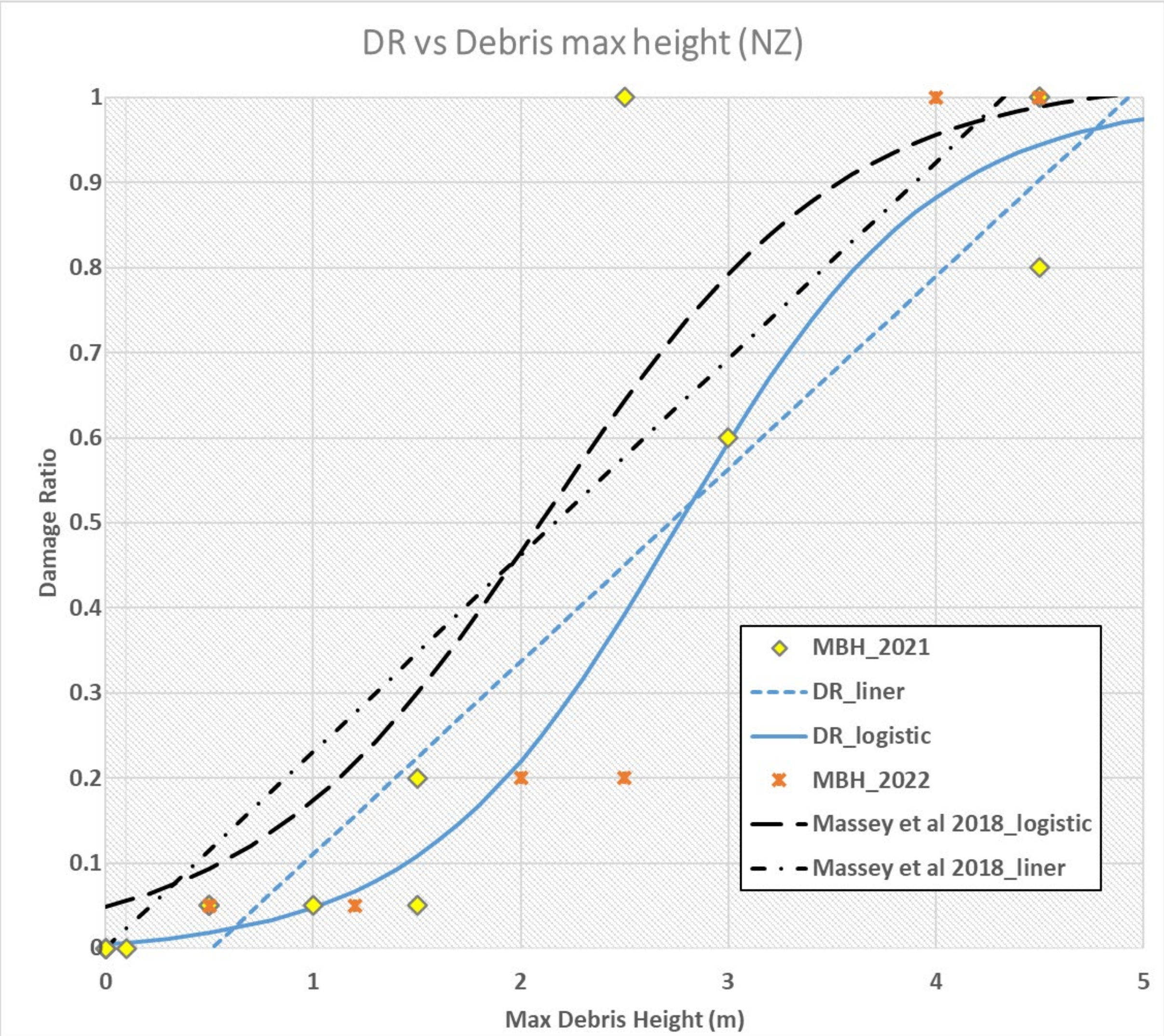

Figure 4.6 Preliminary results of building vulnerability functions from the 2021 and 2022 storm events in the Marlborough Sounds using the relationship between observed damage state and estimated damage ratio.

5.0 DISCUSSION AND CONCLUSIONS

5.1 Rainfall and Landslide Distribution

We have mapped 7597 landslides triggered by the 2021 and 2022 storm events (3792 in 2021 and 3805 in 2022). Below, we discuss factors contributing to the observed landslide distributions, including antecedent rainfall conditions, rainfall, slope angle, geology and land cover. This is a preliminary analysis using available data. For a more thorough analysis, more detailed mapping of near-surface materials (i.e. terrain mapping) is required (see Section 5.3).

Differences in the antecedent rainfall might help to explain differences in the landslide distributions for the 2021 and 2022 storms. Antecedent conditions in August 2022 were wetter than those in 2021 for representative MDC rain gauge stations in the Marlborough region (Figure 5.1), particularly at Kenepuru Head and Wakamarina (~100 mm in the 12 days before the 2022 storm). The Tunakino rain gauge had the highest cumulative rainfall from 2021 to 2023, receiving >7600 mm in the 2.5-year period, whereas Kaituna received the lowest rainfall with ~3800 mm over 2.5 years. During the 2021 storm event, Top Valley received the highest peak daily and total rainfall at 326 mm. During the 2022 storm event, the Tunakino station recorded the highest peak daily and total rainfall (1126 mm). The higher antecedent and storm rainfall amounts, as well as longer storm duration, in 2022 could in part explain the higher occurrence of ground cracking (incipient landsliding) and relict landslide re-activations observed in 2022 (see also Section 5.2).

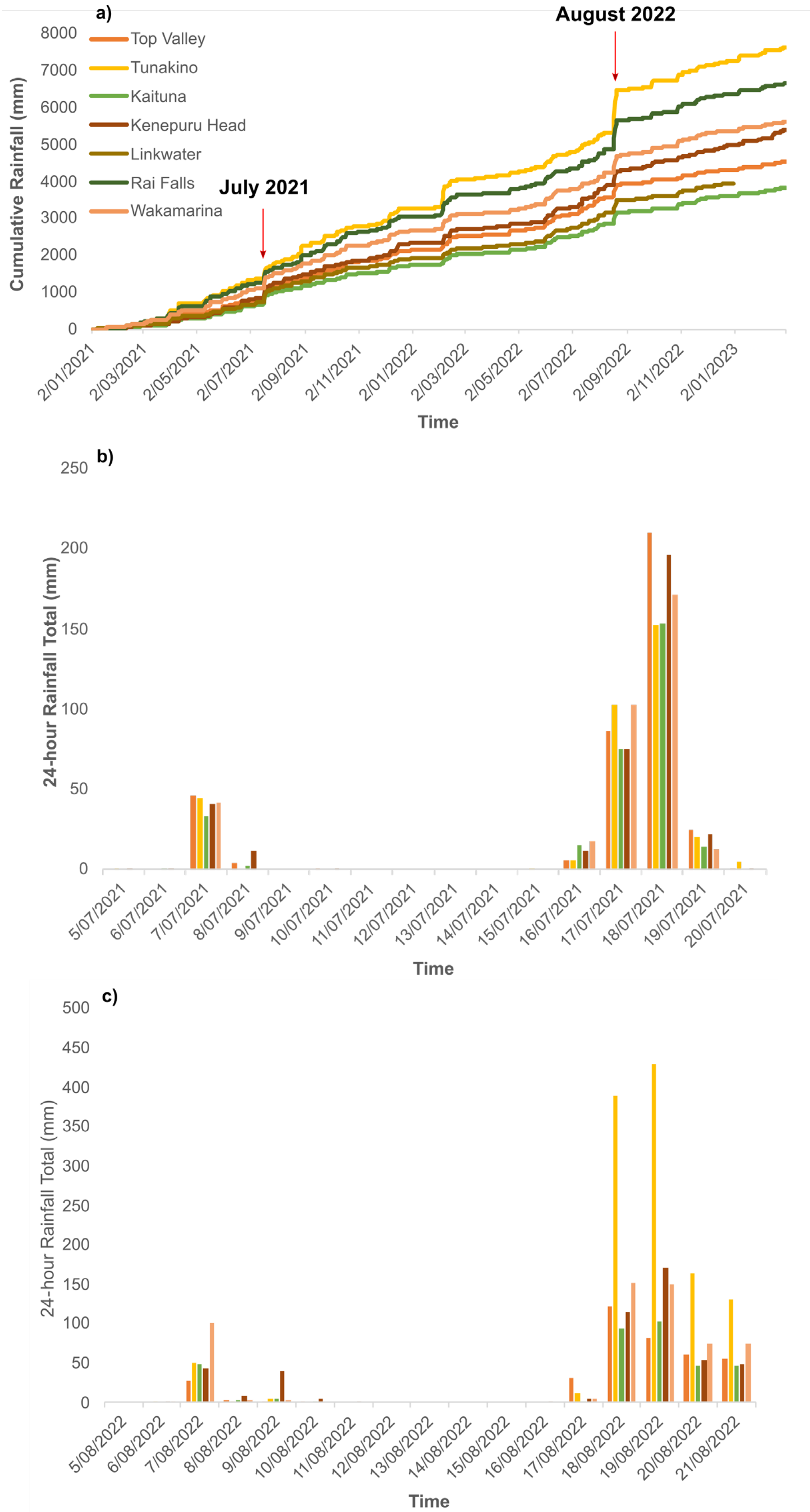

Figure 5.1 Antecedent and storm rainfall at seven stations in the Marlborough region (Top Valley, Tunakino, Kaituna, Kenepuru Head and Wakamarina rain gauges). (a) Cumulative rainfall from 2021 to 2023, with the two storms indicated. (b) and (c) Daily rainfall amounts for the stations in 2021 and 2022, respectively, including two weeks prior to each storm and the storm events (rainfall on the right of the graphs). Note that Rai Falls and Linkwater were excluded from (b) and (c), as they were similar to other gauges. (Data: MDC 2023, pers. comm.).

Storm total rainfall thresholds for ≥1.5 LS/km^2 landslide density in the July 2021 storm were 150–350 mm over the storm duration (54 hours) and 250–400 mm over 96 hours in August 2022. This correlates to an average of 67–178 mm over 24 hours (for two consecutive days) and 63–100 mm over 24 hours (for three days), respectively. Areas receiving >178 mm in 24 hours in 2021 comprised only 3% of the total study area, and 2.2% of landslides occurred on slopes receiving high rainfall amounts. Areas receiving >100 mm in 24 hours in 2022 comprised 50% of the total study area, but only 30% of landslides occurred in these areas. Maximum 24-hour rainfall (based on rain radar) was significantly higher than the average – 379 mm in 2021 and 466 mm in 2022. Landslides occurred disproportionally in areas that received 100–200 mm maximum rainfall in 24 hours in 2021 and 100–400 mm in 2022. Thus, proportionally, more landslides occurred in areas with lower rainfall during both storms. For both storms, the greatest number and density of landslides did not occur in the areas that received the highest rainfall.

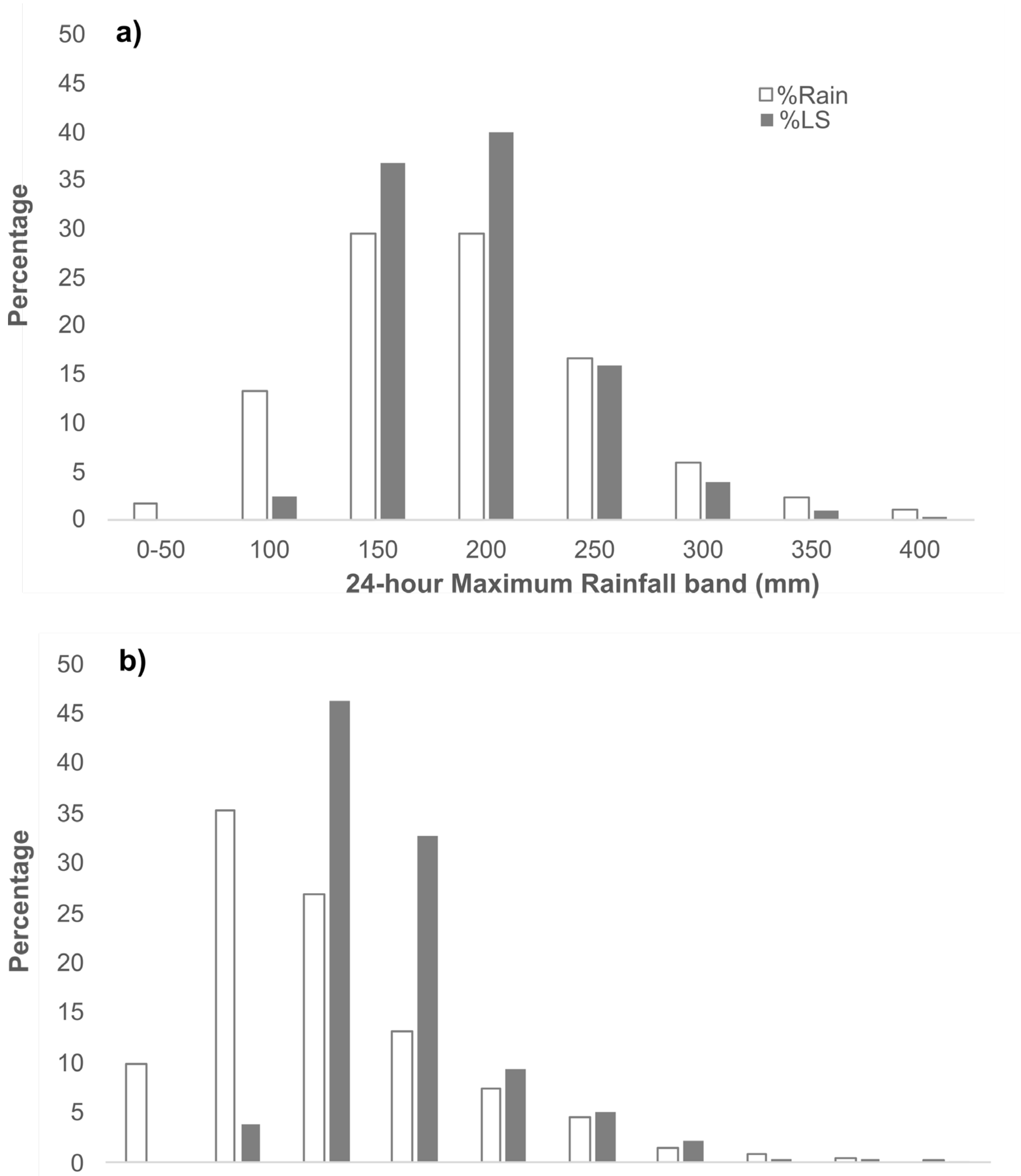

Figure 5.2 Maximum 24-hour rainfall over the study area in (a) 2021 and (b) 2022, showing the percentage of areas that received rainfall in each band and the percentage of landslides initiated in those rainfall bands.

Landslide distributions in July 2021 and August 2022 do not seem to be controlled by the rainfall distribution alone.

- In both storms, landslides most frequently occurred on slopes between 20° and 50°. Median slope angle values for most geological units and almost all land-cover classes were consistently 38° ± 3°.
- In July 2021, many landslides (1889, or 50%) occurred in areas of plantation forestry or recently harvested forestry and on slopes underlain by Rakaia Terrane schist (TZIIIB-IV) or Waipapa Composite Terrane semi-schist (TZIIA). The highest landslide density (>10 LS/km^2) was also in harvested forest. It seems that the combination of forestry on slopes underlain by metamorphosed bedrock is more susceptible to landsliding.
- In August 2022, most landslides (2385, or 63%) occurred in areas of pasture and scrub in TZIIA Caples and Waipapa Composite semi-schist and Pleistocene–Holocene sediments. The percentages of landslides in plantation forests and harvested forests were lower than in 2021. The highest landslide density was in Brook Street Terrane tuffaceous sandstones and siltstones, although landslides were widespread across a variety of rock types and were probably controlled by the distribution of surficial materials, such as colluvium and regolith (not mapped).

A possible significant factor in explaining the 2021 versus 2022 landslide distributions is the different spatial distributions of the storms. Although some of the heaviest rain fell on higher elevation slopes covered by indigenous forest in both storms (the Richmond Ranges), with lower landslide densities and higher rainfall values, heavy rain also fell on plantation forestry and recently logged areas in 2021 but not in 2022. The steep hill country of the Northbank area, along the northern side of the Wairau River, was particularly impacted in 2021 due to high rainfall on steep slopes composed of weathered surficial material underlain by highly metamorphosed rocks where logging and forestry operations were also ongoing (Wolter et al. 2022). In 2022, the heaviest rain fell on the outer Marlborough Sounds, where the land cover was dominated by pasture or scrub, which is typical of historically disturbed and successional vegetation types associated with the reversion from grazed pasture to indigenous forest (LCDB v5 Class Descriptions), as well as high altitude areas with indigenous forest. Our data suggest that pasture on slopes >10° (excluding outliers on slopes <10°) at various stages of reversion to indigenous forest and exotic forest (on slopes >15°, excluding outliers) are susceptible to landsliding under heavy rain conditions.

Most of the landslides mapped in both storm events appear to be shallow landslides in highly weathered surficial material, possibly at the interface of regolith and bedrock, and colluvium. Some were also re-activations of larger, deeper-seated relict landslides in bedrock, particularly in the Caples Terrane. Clusters of shallow, smaller landslides also occurred within some of the relict ones (within landslide debris).

The parent rock determines some of the characteristics (strength, plasticity, etc.) of the surficial weathered material derived from it. This is seen most clearly in the relationship between Pleistocene–Holocene sediments and bedrock. Most (68%) Pleistocene–Holocene sediments in the study area are relict landslide deposits, and the remaining 32% are fan (28%) and alluvial terrace (5%) deposits. Of these relict landslides, 79% occur within Caples Terrane parent material, 19% in Rakaia schist and 5% in Waipapa semi-schist. Landslides occurred in Caples Terrane semi-schist and Pleistocene–Holocene sediments with some of the lowest rainfall amounts compared to other geological units in both storms, and over half of the landslides occurred in these two geological groups (55%). This indicates that relict landslides in underlying Caples Terrane are particularly susceptible to landslide re-activation (both as a whole and as shallower, smaller landslides within larger relict ones), as observed during the 2022 storm. The degree of metamorphism (textural zones) could play a role in landslide susceptibility, but our data do not present a clear pattern. Current and historic land cover and rainfall certainly exacerbate slope instability.

5.2 Landslide Behaviour and Mobility

A notable difference from the July 2021 storm was the amount of ground cracking, or signs of incipient landsliding, that occurred in August 2022. For the landslides we visited for detailed site investigations, there were fewer debris flows and more slumps and slides. This difference could be related to antecedent ground conditions and the rainfall amount, intensity and duration. The 2022 storm re-activated more large, relict landslides, generating ground cracking (incipient landsliding). This is likely related to antecedent ground conditions – August 2022 was wetter before the storm than July 2021 (see Section 4.1).

The landslides visited in the field in August 2022 were less mobile than average literature values (above the mean line in Figure 5.1) and smaller than the July 2021 sites visited (to the left on Figure 5.1).

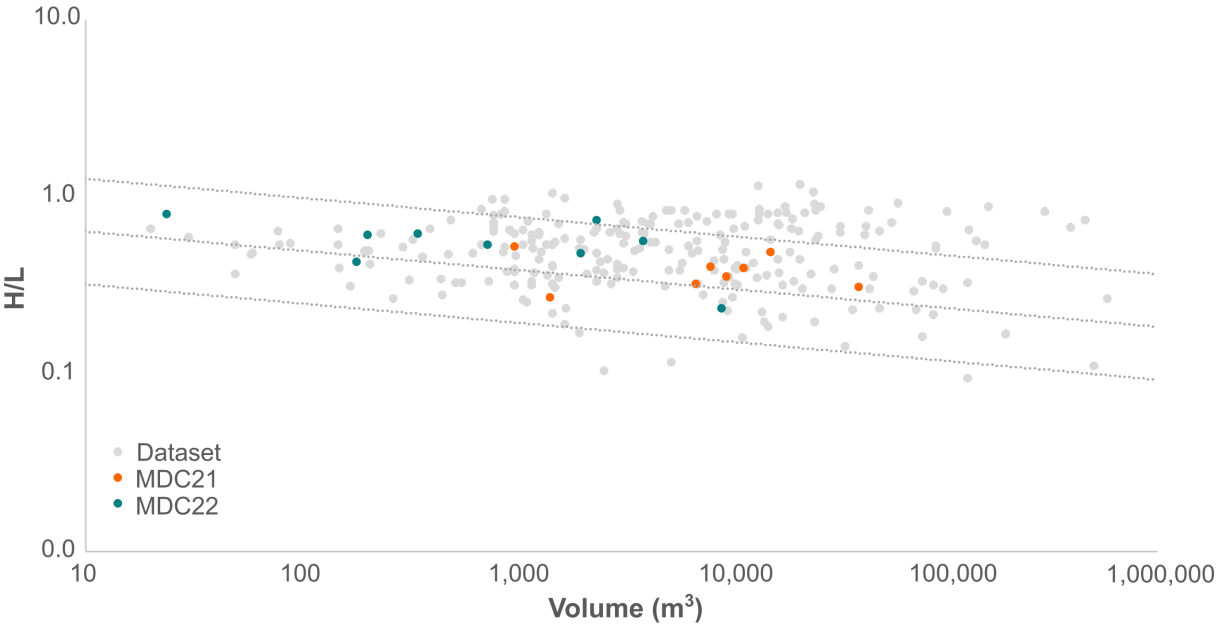

Figure 5.3 Mobility plot of debris trail volume versus landslide height / steepest path distance. Global dataset shown in light grey, with mean, -2 standard deviation and +2 standard deviation curves. July 2021 sites visited are in orange and August 2022 sites visited are in teal. H/L: height (H) of landslide (crown to toe elevation difference) over landslide travel distance / runout (L).

5.3 Building Damage

Over the two-day period that site visits were conducted following the August 2022 storm, nine buildings were surveyed with structural attributes recorded. The damage state of building structures, non-structures, contents and stocks replacement costs were quantified where possible. Similarly, the affected habitability of building was noted in many cases.

All buildings surveyed were residential with timber construction. Observed building damage states were evenly distributed from no damage (DS0) to critical damage (DS5), reflecting the site selection rationale for this study. These ground investigation surveys aimed to enhance the understanding of how New Zealand building assets are damaged by landslide hazard (e.g. debris flows) generated during rainstorm events. In this study, we found that when debris height is greater than 1.5 m (or debris cross-sectional areas are greater than 55% of the building wall area), it resulted in moderate to critical damage to buildings. Landslide debris caused much damage to buildings (Figure 5.2). Debris (including vegetation) damaged windows and house walls, and, in some cases, compromised building integrity (i.e. collapse).

Among the nine surveyed buildings, three of them were classified as R2 colour tagging (namely: entry prohibited, severe damage to building). They were either buried or destroyed by debris (Figure 5.2) or collapsed. Although there was severe damage to these buildings, no death or injury occurred, as the houses were vacant during the event.

Figure 5.4 Damage to a building from large debris flow.

The empirical building damage data described in this report is intended to support the future development of landslide vulnerability models for New Zealand buildings. The vulnerability models will represent building damage response (i.e. damage ratio) to increasing landslide intensity (e.g. debris flow depth). The damage ratio is calculated as repair cost / replacement value. We are still waiting for building claim information (from Toka Tū Ake EQC) to determine the repair cost, hence we are unable to calculate the damage ratios of the surveyed buildings at this time.

Note that it was difficult and impractical for the field team to determine the building repair cost on the ground. However, we were able to capture the building damage state and gain a preliminary understanding of building performance from the recent landslide events in the Marlborough Sounds based on the recorded damage state of the surveyed buildings, along with the suggested damage ratio as shown in Table 4.2 and Figure 4.6.

The preliminary vulnerability models are expected to be refined once building insurance claim information (hence repair cost) becomes available. The improved building vulnerability functions can then be applied in risk modelling software to estimate the potential impact and loss sustained by landslide hazards in future storm events.

5.4 Recommendations

- Most landslides, regardless of geology or land-cover class, occurred on slopes with median angles of ~38°. Minimum landslide slope angles as low as 10° (excluding outliers) were observed, particularly for pasture. We recommend monitoring pasture and exotic forestry on slopes >10–15° after significant rainfall (>100 mm/day for 2–3 days) for landslide activity. Although more analysis is required, similar values could be used to develop landslide TARPs (trigger action response plans) in future.
- Map the distribution and depth of near-surface materials in detail to have a better understanding of the roles that soil, regolith, colluvium and bedrock play in landslide initiation. Our observations have pointed to the potential role of thick colluvium and regolith as a landslide susceptibility factor. It is not currently possible to statistically evaluate the role of these due to insufficient information of their distribution. Therefore, mapping the distribution and depths of these may be useful for helping to refine susceptibility models in the future.
- Investigate landslide type and size relative to slope angle, rainfall, land cover and geological unit to further analyse any possible thresholds (requires landslide polygons) (Action for GNS Science).
- Update the LCDB for all land-cover classes, as was done in this study for exotic forest / harvested forestry in 2021 and 2022. Many relict landslides, particularly Pleistocene–Holocene landslides in Caples Terrane, were re-activated during the August 2022 storm event. It would be beneficial to identify and map relict landslides in the Marlborough Sounds to identify slopes that have been unstable in the past and could re-activate in future extreme rainfall events.
- Monitor areas with high ground-cracking density, especially in areas with residential dwellings – further landslides could occur in these areas, particularly in future storms. Site investigations may be required to determine appropriate monitoring methods.
- This report evaluated the roles of single susceptibility variables. However, landslide susceptibility is a multi-variate issue and requires multi-variate statistical techniques to forecast landslide impacts. Data collected as part of this project will be used to train the Rainfall-Induced Landslide (RIL) forecast tool, a multi-variate statistical susceptibility tool developed by GNS Science, for the Marlborough region (Action for GNS Science). We suggest a discussion between GNS Science and MDC to tailor the RIL model and tool for the Marlborough region.
- Refine the landslide vulnerability models for New Zealand buildings, once the insurance claims from Toka Tū Ake EQC become available, as part of other on-going landslide research projects led by GNS Science (Action for GNS Science). Again, discussions between GNS Science and MDC would be recommended to ensure applicability in the Marlborough region.
- This report and Wolter et al. (2022) document 18 selected landslide sites where dwellings were impacted, with many others not inspected for logistical and cost reasons. To date, no injury or loss of life has occurred at any sites, but significant property damage has occurred and risks from landslides are evident in the Marlborough Sounds. This report is well supported by numerous historic council and published studies. We recommend a quantitative analysis of the risks posed by landslides in this area. Such investigation should include application of the RIL forecast tool in combination with landslide runout analyses and engineering data on dwellings. GNS Science can provide examples of similar risk analyses completed for other district and regional councils.

6.0 ACKNOWLEDGMENTS

MDC and GeoNet co-funded the joint MDC / GNS Science event response. We gratefully acknowledge the support of MDC, and Matt Oliver in particular, who organised field logistics and undertook fieldwork with the GNS Science team. We also thank Sam McColl and Regine Morgenstern for reviewing the report internally.

7.0 REFERENCES

Building Performance. [2023]. Managing buildings in an emergency. Wellington (NZ): Ministry of Business, Innovation & Employment; [accessed 2023 Jun]. https://www.building.govt.nz/managing-buildings/managing-buildings-in-an-emergency

Heron DW, custodian. 2020. Geological map of New Zealand: digital vector data [map]. 3rd ed. Lower Hutt (NZ): GNS Science. 1 USB, scale 1:250,000. (GNS Science geological map; 1).

Hungr O, Leroueil S, Picarelli L. 2014. The Varnes classification of landslide types, an update. *Landslides*. 11(2):167–194. doi:10.1007/s10346-013-0436-y.

[LINZ] Toitū Te Whenua Land Information New Zealand. 2012. NZ 8m Digital Elevation Model (2012). Wellington (NZ): LINZ; [updated 2022 Jun 29; accessed 2023 Jun]. https://data.linz.govt.nz/layer/51768-nz-8m-digital-elevation-model-2012/

Lucieer A, Jong SMd, Turner D. 2013. Mapping landslide displacements using Structure from Motion (SfM) and image correlation of multi-temporal UAV photography. *Progress in Physical Geography: Earth and Environment*. 38(1):97–116. doi:10.1177/0309133313515293.

Massey CI, McSaveney MJ, Taig T, Richards L, Litchfield NJ, Rhoades DA, McVerry GH, Lukovic B, Heron DW, Ries W, et al. 2014. Determining rockfall risk in Christchurch using rockfalls triggered by the 2010–2011 Canterbury earthquake sequence. *Earthquake Spectra*. 30(1):155–181. doi:10.1193/021413eqs026m.

Massey CI, Thomas K-L, King AB, Singeisen C, Taig T, Horspool NA. 2019. SLIDE (Wellington): vulnerability of dwellings to landslides (Project No. 16/SP740). Lower Hutt (NZ): GNS Science. 76 p. (GNS Science report; 2018/27). doi:10.21420/G2DD2Q.

Massey CI, Townsend DB, Leith K, Rosser BJ, Farr J. 2022. GeoNet landslide response: Nelson-Tasman District, 16–19 August 2022. Lower Hutt (NZ): GNS Science. 25 p. (GNS Science report; 2022/58). doi:10.21420/N4R1-Q533.

[NZGS] New Zealand Geotechnical Society. 2005. Field description of soil and rock: guideline for the field classification and description of soil and rock description for engineering purposes. [Rev. ed.]. Wellington (NZ): New Zealand Geotechnical Society. 38 p.

Rosser BJ, Townsend DB, Oliver M. In prep. GeoNet landslide response: Marlborough District, 16–19 August 2022. Lower Hutt (NZ): GNS Science. (GNS Science Report; 2022/30). doi:10.21420/TKNZ-9G59.

Wolter A, Rosser BJ, Lin S-L, Boyes AF, Townsend DB, Jones KE, Choi E. 2022. Phase I: reconnaissance report on landslides caused by the 16–18 July 2021 rainstorm in the Marlborough region. Lower Hutt (NZ): GNS Science. 68 p. (GNS Science report; 2022/08). doi:10.21420/C7DK-BQ35.

APPENDICES

This page left intentionally blank.

APPENDIX 1 LANDSLIDE DETAILS

Table A1.1 Landslide details. H/L: height (H) of landslide (crown to toe elevation difference) over travel distance (L).

Landslide ID	Landslide Type	Impact Type	Max Debris Height (m)	Source Area (m^2)	Debris Trail Area (m^2)	Source Volume (m^3)	Scour Volume in Debris Trail (m^3)	Debris Trail Volume (m^3)	% Entrained	Height (m)	Travel Distance (m)	H/L
22-1	Debris spread/flow	Debris inundation	1.6	44.3	35.5	58.0	-	23.7	-	12	15.1	0.81
22-2	Debris flow/flood	Debris inundation	4.2	1068.1	3317.9	2470.6	1639.9	2017.5	-	148	265.4	0.49
22-3	Retrogressive slump	Slippage	N/A	1623.0	2181.2	3146.7	-	3955.1	1.2	60	86.6	0.57
22-4	Rotational slide	Debris inundation	1.5	1718.3	2174.1	2365.3	-	2406.4	1.1	78	80.8	0.75
22-5	Debris flow	Debris inundation	2.5	1603.7	10527.9	3901.6	1802.2	9178.7	2.4	136	465.1	0.24
22-6	Debris slump/slide	Slippage	N/A	661.5	697.2	970.2	-	353.6	-	33	50.7	0.63
22-7	Debris slump/flow	Debris inundation	3.3	196.2	335.4	101.7	19.8	183.5	1.8	27	58.2	0.44
22-8	Debris avalanche	Debris inundation	1.0	1740.9	1691.2	1306.0	39.1	747.2	-	69	117.1	0.54
22-9	Debris slump/slide	Slippage	N/A	178.3	157.9	137.7	-	207.0	-	14	22.6	0.62

APPENDIX 2 RPAS MAPS AND 3D MODELS

A2.1 Links to 3D Models of Landslides

3D models generated from the UAV surveys can be viewed on the GNS Science Sketchfab webpage. These models are private; only those with the link can see them. The Sketchfab models have a lowered resolution to optimise them for viewing over the internet.

- Landslide ID 1: https://sketchfab.com/3d-models/marlborough-landslide-2022-4aeb893d19114d6881d0825cd47fc9a3
- Landslide ID 2: https://sketchfab.com/3d-models/marlborough-landslide-2022-feea1cc5639a47ddb51969294850f2c2
- Landslide ID 3: https://sketchfab.com/3d-models/marlborough-landslide-2022-c3d0e316f0a0434bbaba14507b242ae4
- Landslide ID 4: https://sketchfab.com/3d-models/marlborough-landslide-2022-d86f14d82fed4e4ea715f4775d537b64
- Landslide ID 5: https://sketchfab.com/3d-models/marlborough-landslides-2022-d45e93737e4c427e8f5b9fd76c154cfa
- Landslide ID 6: https://sketchfab.com/3d-models/marlborough-landslides-2022-006ce55d16a64e4bb2c1b6814adeabd5
- Landslide ID 7: https://sketchfab.com/3d-models/marlborough-landslide-2022-79dd09af4f76484b86caf0eee0e7a99e
- Landslide ID 8: https://sketchfab.com/3d-models/marlborough-landslides-2022-134b4dd2253b4867baa0d8ce9b1fbc63
- Landslide ID 9: https://sketchfab.com/3d-models/marlborough-landslide-2022-111c4038f83a4c0da1746554f978b792

A2.2 Orthomosaics, Digital Surface Models and Erosion and Deposition Maps (Difference Models)

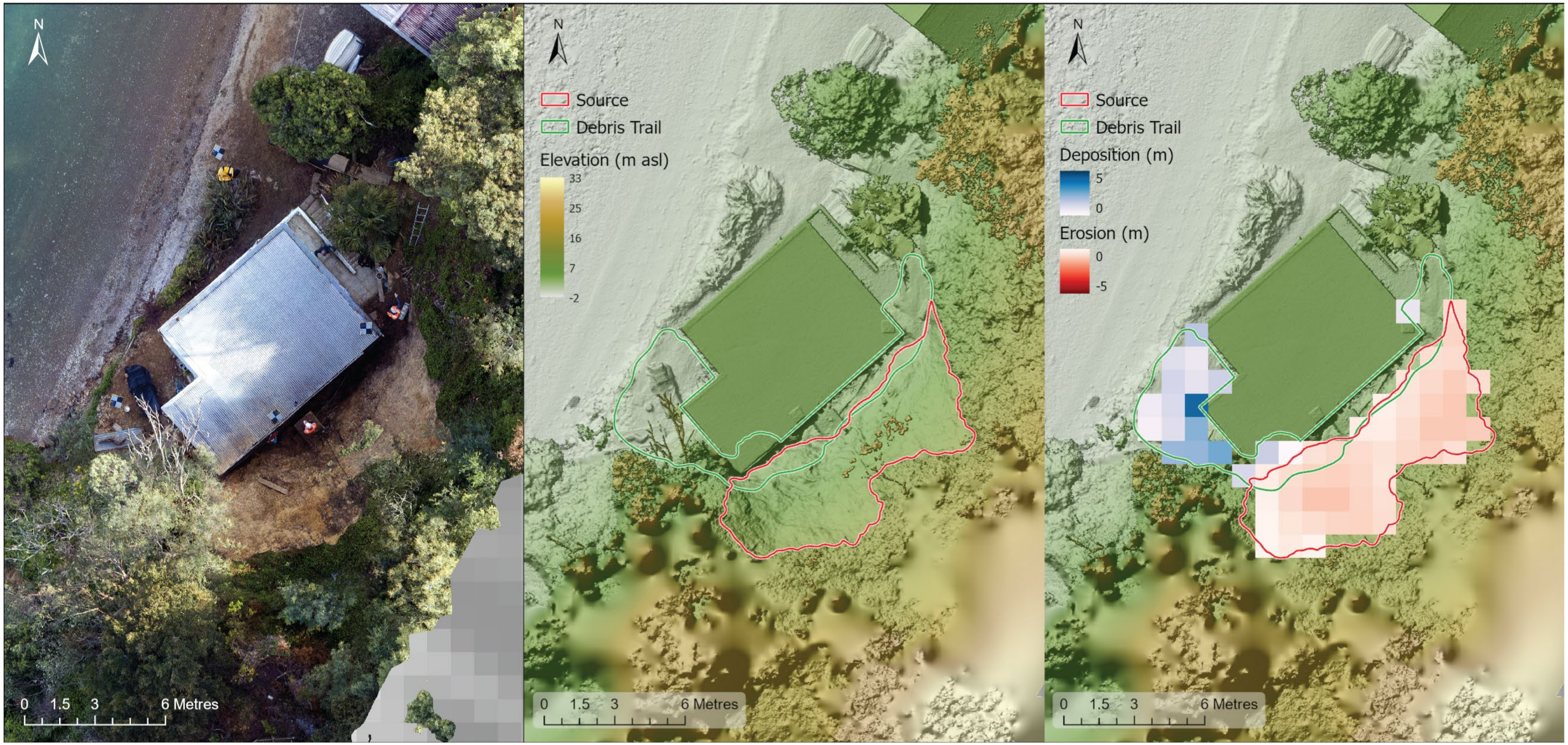

Figure A2.1 Landslide ID (LSID) 22-1 RPAS maps. Left: orthomosaic. Middle: Digital Surface Model. Right: Erosion and deposition.

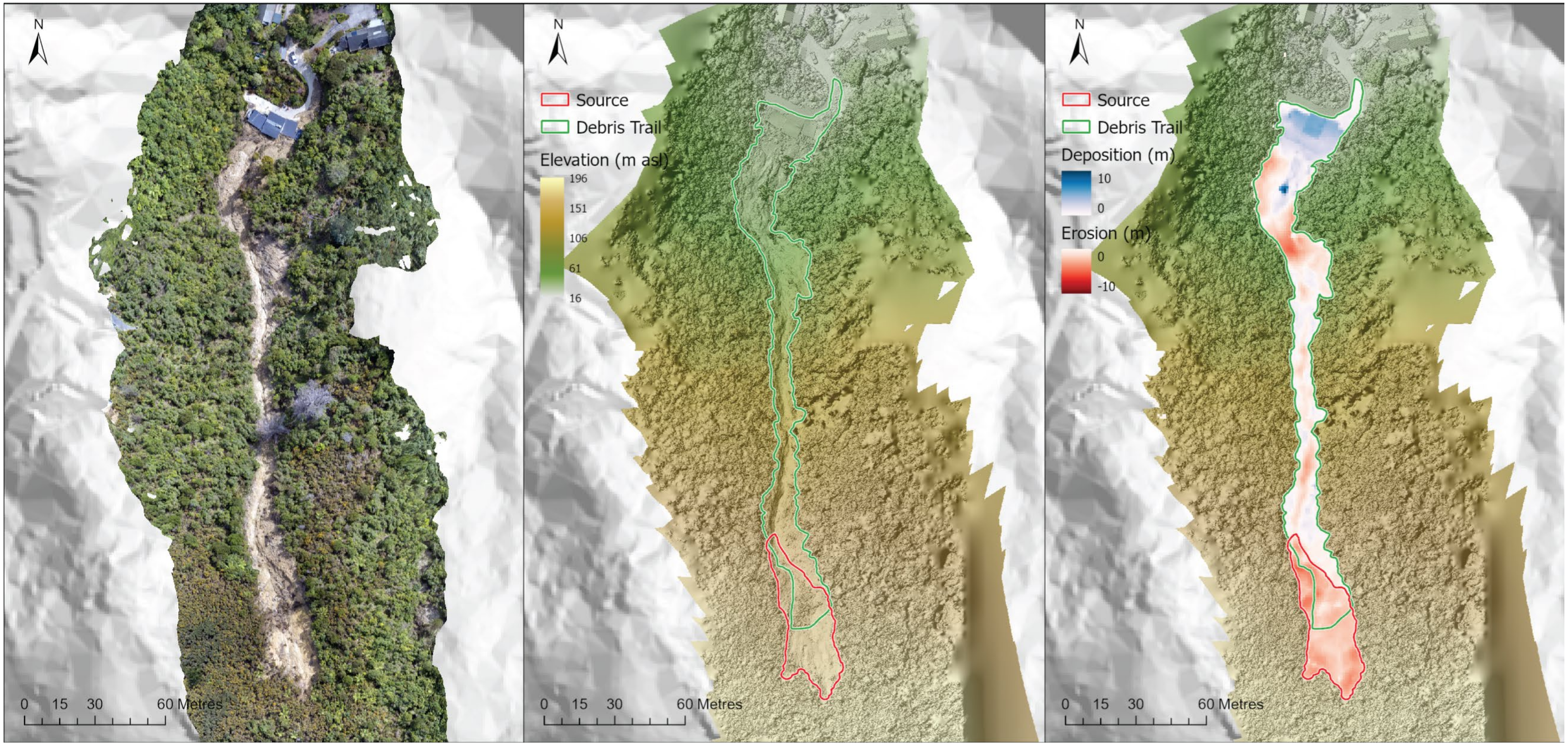

Figure A2.2 LSID 22-2 RPAS maps. Left: orthomosaic. Middle: Digital Surface Model. Right: Erosion and deposition.

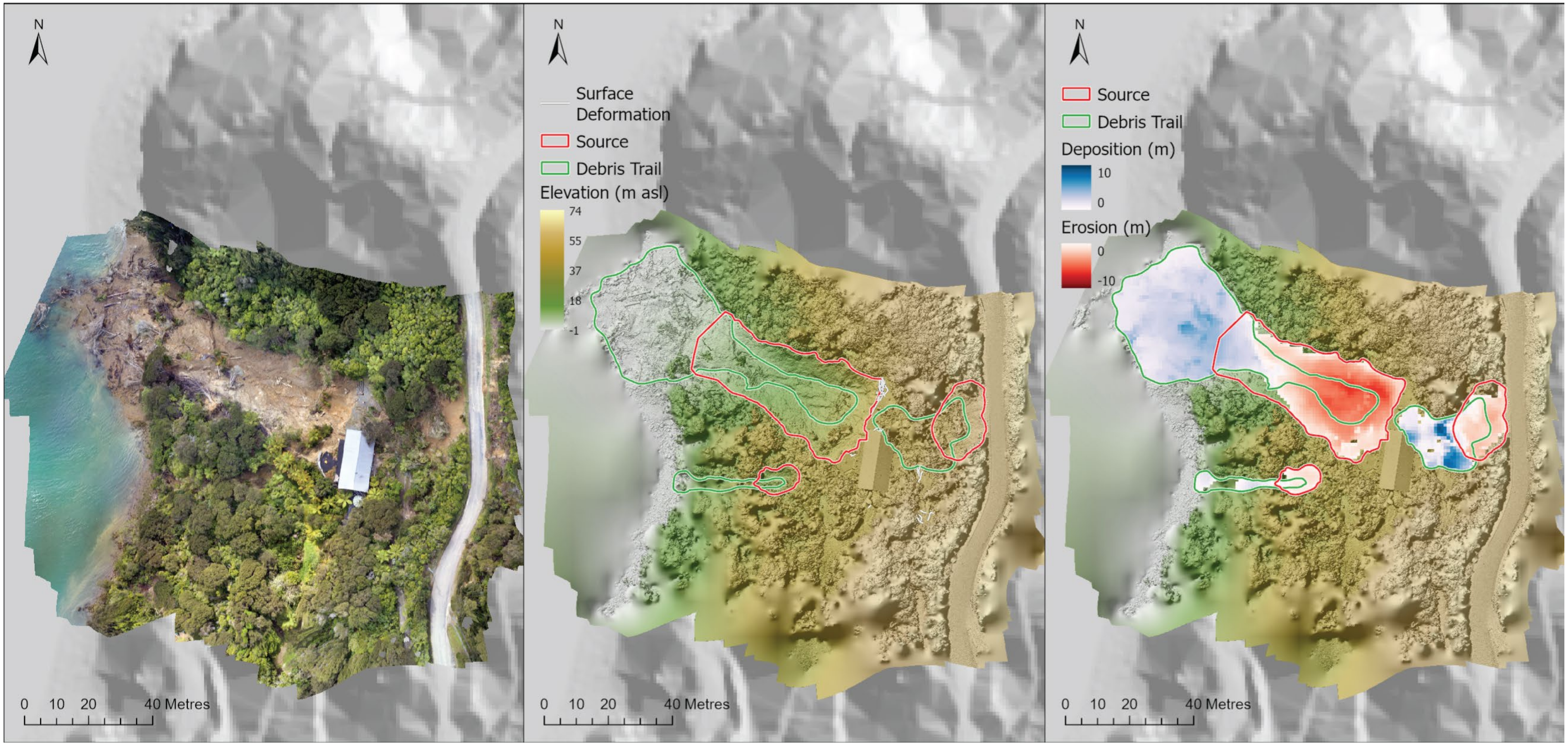

Figure A2.3 LSID 22-3 RPAS maps. Left: orthomosaic. Middle: Digital Surface Model. Right: Erosion and deposition.

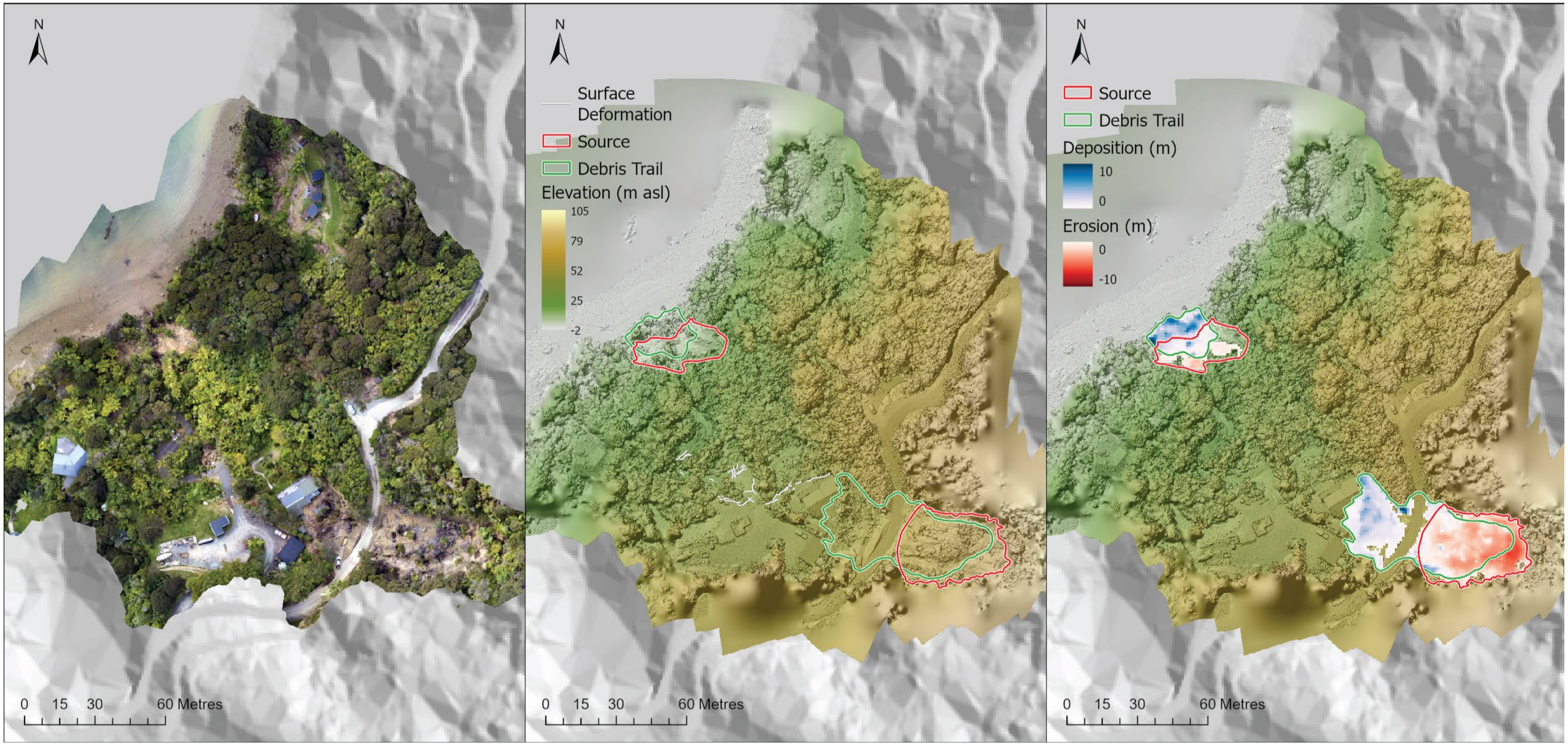

Figure A2.4 LSID 22-4 RPAS maps. Left: orthomosaic. Middle: Digital Surface Model. Right: Erosion and deposition.

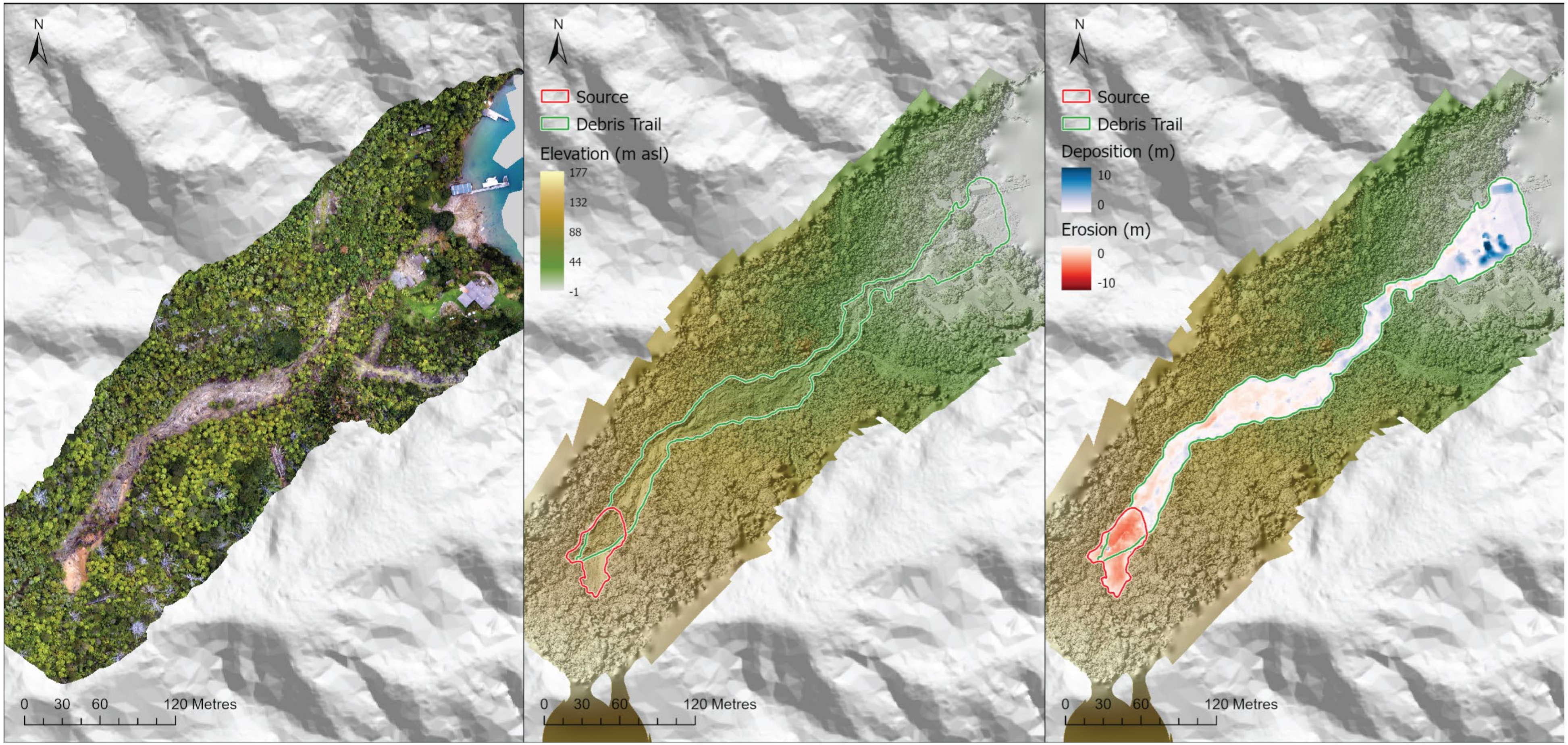

Figure A2.5 LSID 22-5 RPAS maps. Left: orthomosaic. Middle: Digital Surface Model. Right: Erosion and deposition.

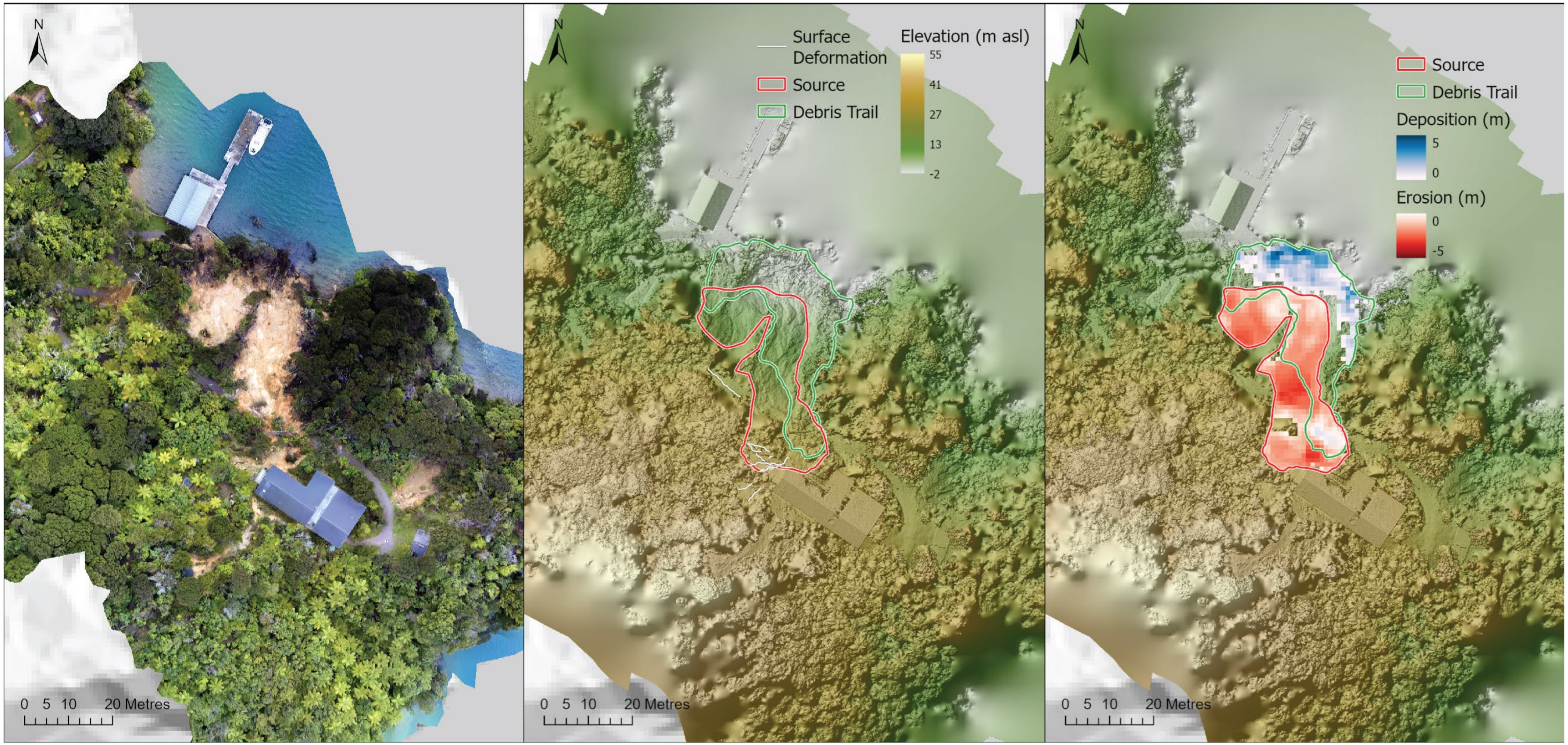

Figure A2.6 LSID 22-6 RPAS maps. Left: orthomosaic. Middle: Digital Surface Model. Right: Erosion and deposition.

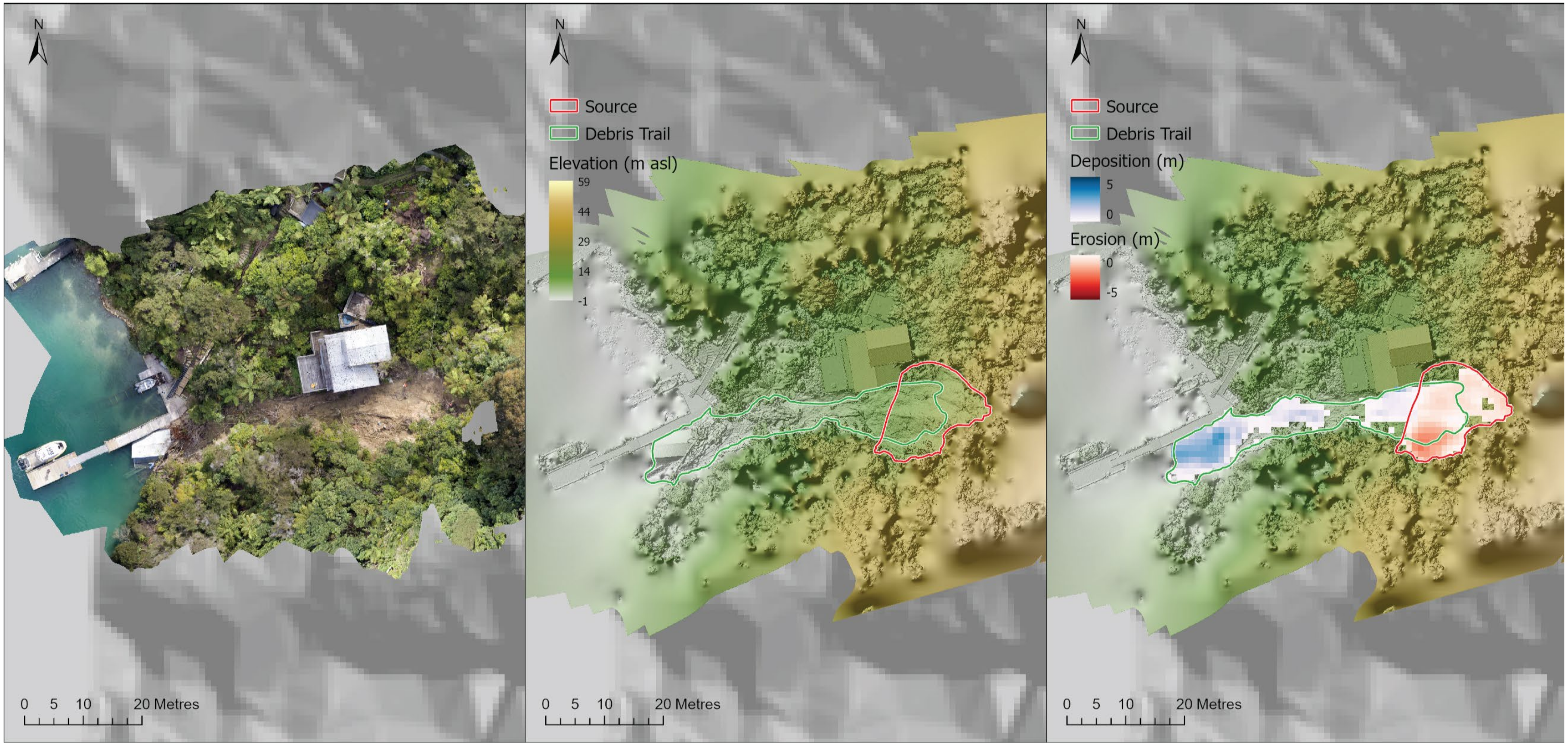

Figure A2.7 LSID 22-7 RPAS maps. Left: orthomosaic. Middle: Digital Surface Model. Right: Erosion and deposition.

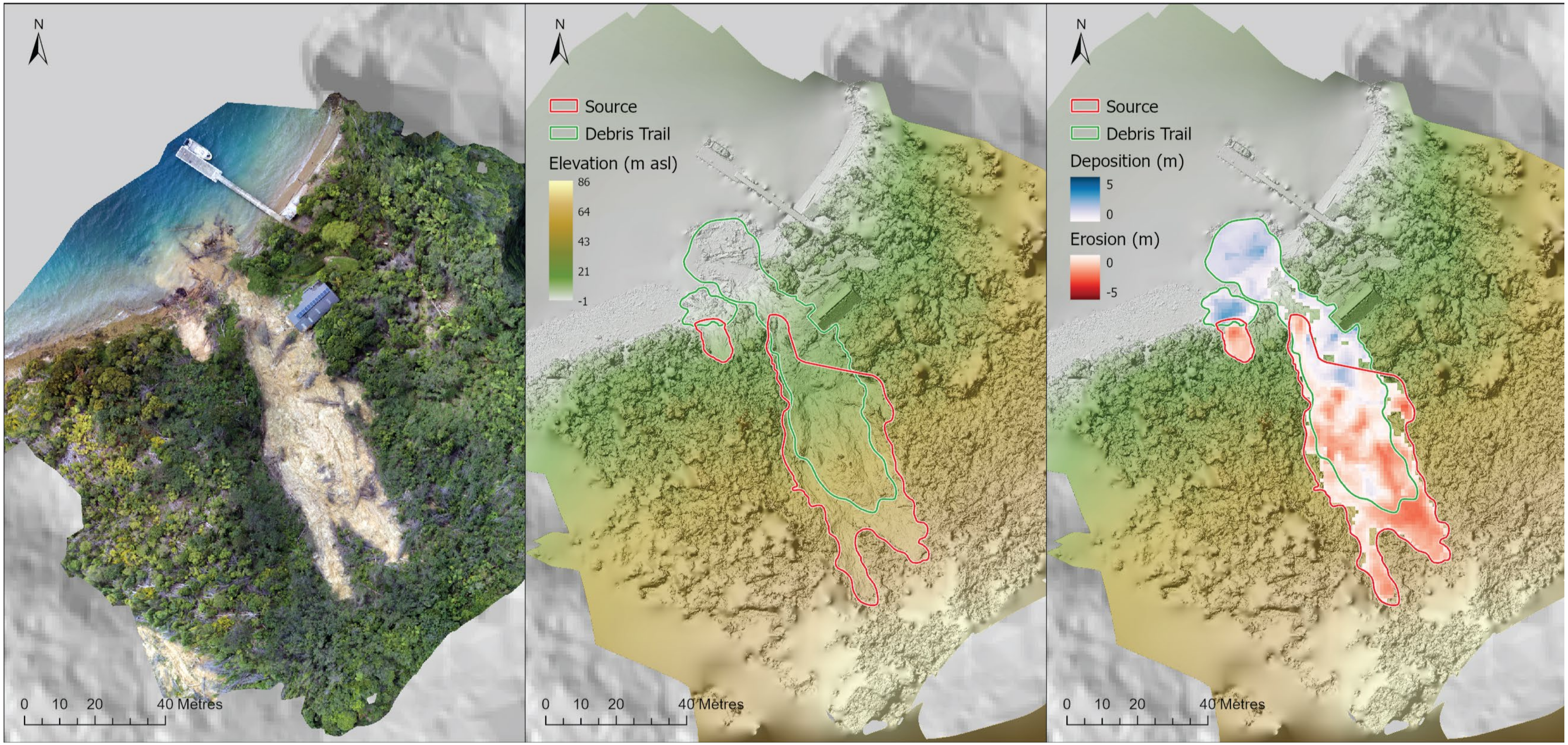

Figure A2.8 LSID 22-8 RPAS maps. Left: orthomosaic. Middle: Digital Surface Model. Right: Erosion and deposition.

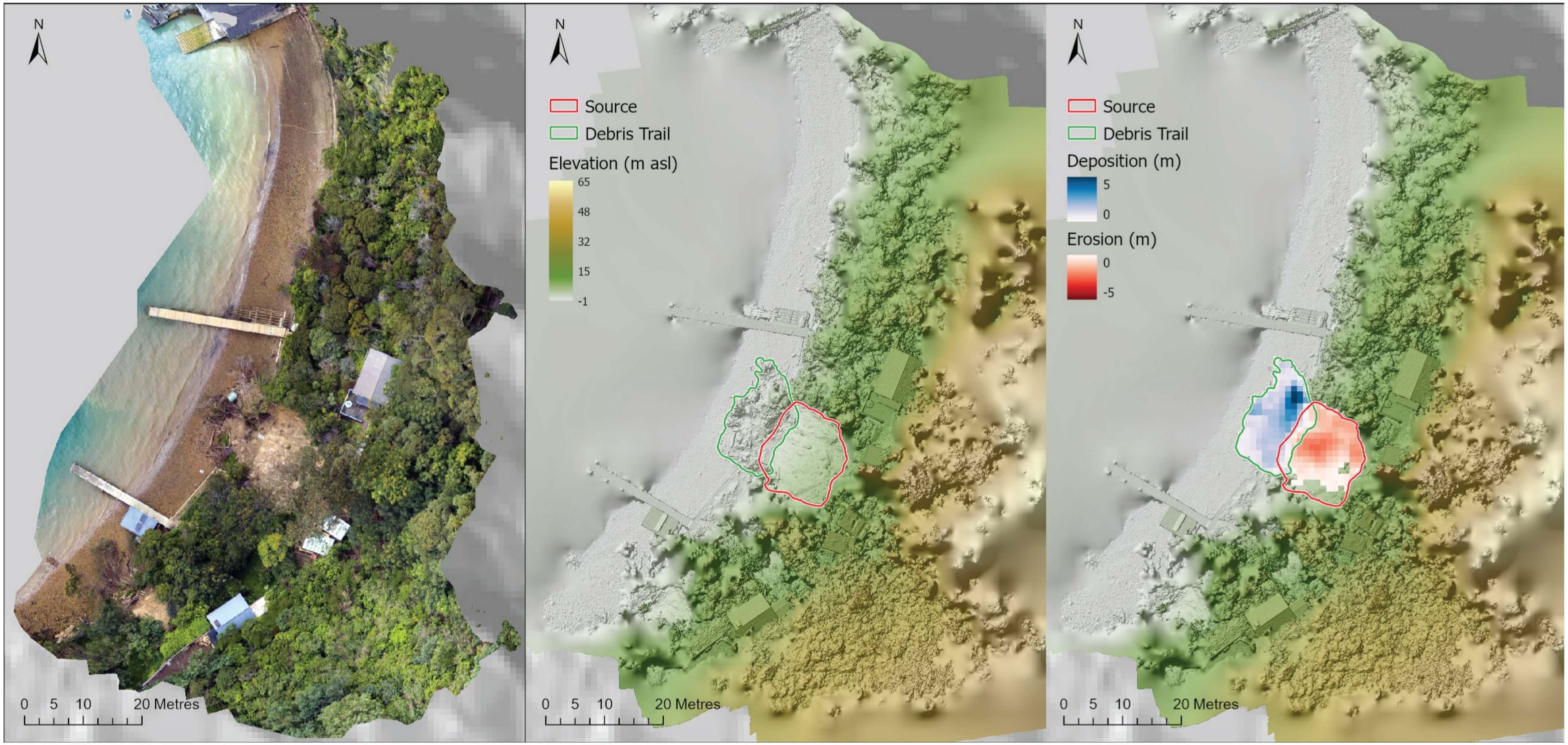

Figure A2.9 LSID 22-9 RPAS maps. Left: orthomosaic. Middle: Digital Surface Model. Right: Erosion and deposition.

APPENDIX 3 BUILDING DAMAGE SURVEY DATA COLLECTION TEMPLATE

Prepared by: Andrea Wolter, Sheng-Lin Lin (GNS Science)

The following presents the ideal collection of data or 'wish list' related to buildings impacted by landslides. Collecting these data ensures that landslide damage is documented so that losses (impacts) can be analysed adequately. Note that these are based on Massey et al. (2019) and Wolter et al. (2022). Please refer to the respective reports for further details.

A3.1 RPAS Survey

- High-resolution photogrammetric/LiDAR/other survey.
- Output: 3D surface model of landslide (including source to toe, if possible) and buildings impacted (see Figure A3.1).
- See Wolter et al. (2022) for differencing methodology.

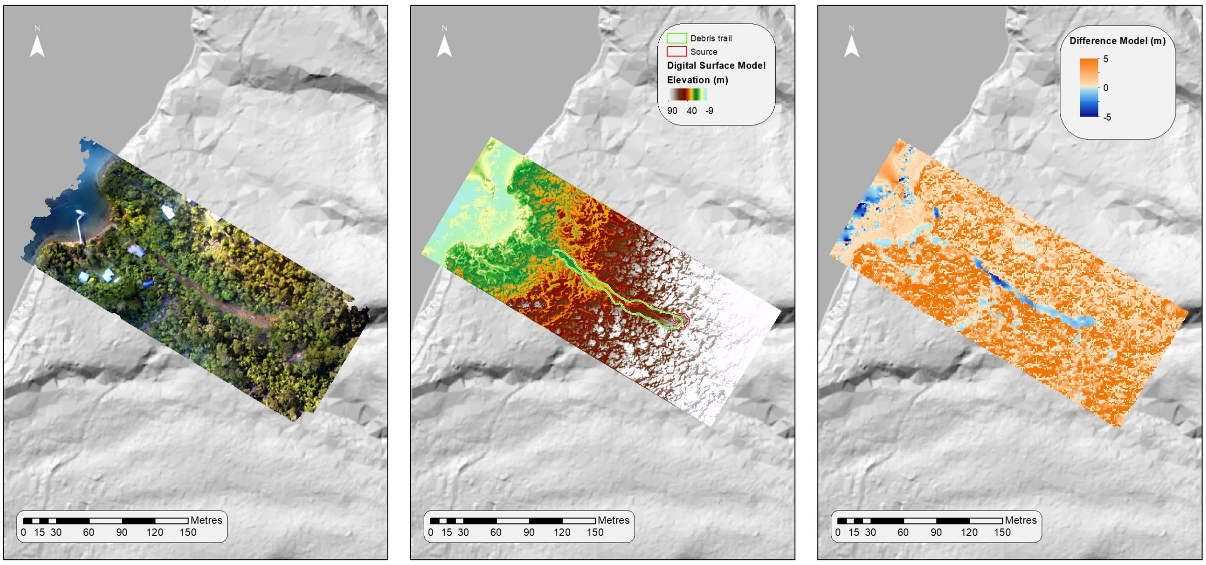

Figure A3.1 Example of RPAS photogrammetric surveys.

A3.2 Landslide Survey

- Landslide type (based on Hungr et al. [2014]).
- Source area:
  - Source area length, width and depth, area and volume.
  - Source material (according to NZGS [2005] guidelines for material description).
  - Future landslide potential, any tension cracks, etc.
- Debris trail:
  - Travel distance.
  - Landslide height (elevation difference between crown and toe).
  - H/L[6] (vertical angle between crown and toe locations).
- Debris inundation:
  - Maximum height of main deposit against building, including run-up (e.g. Figure A3.2).
  - Cross-sectional area of building impacted by debris.
- Slippage:[7]
  - Magnitude of displacement.
  - Proportion of dwelling moved or undercut by debris movement.

Figure A3.2 Surveying of landslide debris; measuring inundation along building side. We measured maximum run-up signs (here, above the building windows) not the height of the debris at the time of survey (here, at the base of the windows).

6 Height (H) of the landslide (difference between crown and toe of landslide) over the travel distance (L).

7 'Slippage' is defined here as occurring when a landslide undercuts a building.

Date:

Location:

Key landslide data to be collected

Data	Description	Metric
Landslide type and hazard	Classified using Hungr et al. (2014) and whether hazard is falling debris, slippage, or both.	Classification
Source Area		
Length (Ls)	Maximum length of source area (m).	Number
Width (Ws)	Maximum width of source area (m).	Number
Depth (Ds)	Maximum depth of source area (m).	Number
Area	Source area (m^2), estimated as Ls x Ws or calculated from polygon mapping in office.	Number
Volume	Volume of source area (m^3), estimated as Ls x Ws x Ds or calculated from RPAS surveys and polygon mapping in office.	Number
Source material	Source material; use NZGS (2005) for descriptions of rock and soil.	Description
Signs of ongoing/ future instability	Any signs of ongoing or future instability, such as tension cracks or future landslide potential. Estimate/measure crack opening, block dimensions of hanging material, etc.	Description
Debris Trail		
Length (Ld)	Maximum length of debris trail (m).	Number
Width (Wd)	Maximum width of debris trail (m).	Number
Thickness (Td)	Maximum thickness of debris (m).	Number
Area	Area of debris trail (m^2), estimated as Ld x Wd or calculated from polygon mapping in office.	Number
Volume	Volume of source area (m^3), estimated as Ld x Wd x Td or calculated from RPAS surveys and polygon mapping in office.	Number
Debris material	Debris material; use NZGS (2005) for descriptions of rock and soil; note saturation of material, matrix versus clasts, clast size maximum and mode, etc.	Description
Travel distance (L)	Travel distance of the debris (crown to debris toe), estimated in field or calculated in office.	Number
Height (H)	Elevation difference between crown and debris toe, estimated in field or calculated in office.	Number
H/L ratio	Ratio between H and L (H/L).	Number
Debris Inundation		
Max. height (Hm)	Maximum height of debris at building. See over.	Survey
Cross-sectional area	Cross-sectional area of building impacted by the landslide debris. See over.	Number
Slippage		
Displacement	Magnitude of displacement (horizontal and vertical) direction of movement (m, mm and bearing in degrees).	Number
Undercut Percent	Proportion of building moved or undercut by the movement of debris (%).	Number
General		
Photos, sketch	Take photographs; sketch cross-sections and maps of the landslide source and debris trail showing dimensions.	Sketch map

Date:

Location:

Survey of debris height at buildings

Section 1 – typically along back wall of building facing debris.

Distance (m)	Debris Height (m)	Area (m^2)	Comment
0	0	-	-
1	0.2	(distance2 – distance1) x debris height	Any comments on house elements (edge of foundations, walls, height of windows, etc.) or debris (splash height or main deposit, etc.)

Section 2 – typically along side wall of building facing debris.

Distance (m)	Debris Height (m)	Area (m^2)	Comment
0	0	-	-
1	0.2	(distance2 – distance1) x debris height	Any comments on house elements (edge of foundations, walls, height of windows, etc.) or debris (splash height or main deposit, etc.)

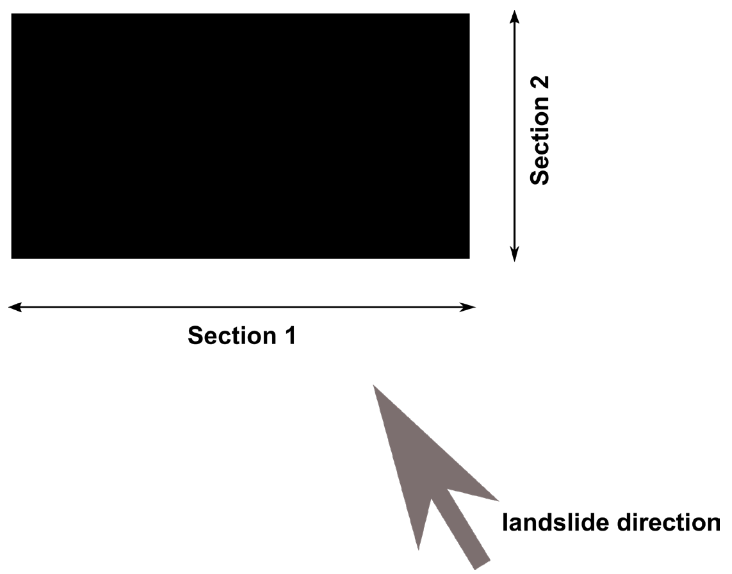

Figure A3.3 Sketch of the two debris-height sections, typically captured along the back (Section 1) and side (Section 2) of a house, facing the landslide debris (represented here as an arrow).

A3.3 Building Survey

Key dwelling data to be collected

Building Attributes	Data to Collect	Metric
ID (address)	-	ID
Building location	Longitude, latitude (NZTM).	Number
Topographic setting	• Flat ground • Flat ground, adjacent to slope: - slope above/below buildings (degree). - slope height (m). - distance to slope (m). • Sloping ground: - Gentle <10°. - Moderate 10–20°. - Steep >20°.	Number
Building use	Residential, dwelling, garage, commercial, others (specify).	Description
Age	Year of original construction and years with major renovations.	Number
Footprint	Footprint area (m^2).	Number
Foundation	Concrete slab, concrete rim/perimeter, rib-raft, timber pile without brace, timber pile with brace, concrete/steel pile.	Classification
Floor Height	Floor height above ground level (m).	Number
Construction / frame type	Timber, brick masonry, concrete masonry, tilt-up panel, advanced design.	Classification
Height	Number of storeys and structure height in metres (m).	Number
Wall cladding	Weatherboard, stucco/roughcast, brick veneer, stone, fibre cement plank, fibre cement sheet, concrete masonry, sheet metal, corrugated iron, etc.	Description
Roof frame	Timber, steel, concrete slab.	Description
Roof slope	Steep (>30°), mild (11–30°), near-flat (1–10°), flat (0°)	Classification
Roof cladding	Sheet metal, clay/concrete tile, metal tile, slate, asphalt and fibreglass shingles, sheet membranes on plywood sheet, concrete, timber	Description
Windows	Number of windows and proportion of house exterior occupied by windows/glass sliding doors	Number
Doors	Number of external doors	Number
Existing placard	**None, W, Y1, Y2, R1, R2**	**Classification**

Other Comment:

Claims information (if available) – land and building costs, imminent risk costs, titles.

Building rapid assessment and sketch sheet

Descriptions and photos/sketches of building damage allow a damage state to be assigned; we are interested in both structural and non-structural damage.

Structural Damage – describe damage to structural elements in the building (e.g. foundation, frame, columns, beams).

Non-Structural – describe superficial damage, e.g. to cladding, gib, floor, roofing, windows, doors, contents.

	RiskScape™ Standard Damage States	GNS Science Damage States
0	**None**: No damage	Damage is outside building footprint
1 (0.2)	**Insignificant:** Minor non-structural damage	Superficial (non-structural) inundation or <10% of building footprint is undercut
2 (0.4)	**Light:** Non-structural damage only	Superficial (non-structural) inundation or <10% of building footprint is undercut
3 (0.6)	**Moderate:** Reparable structural damage.	Structural damage, or house is displaced
4 (0.8)	**Severe:** Irreparable structural damage.	Structural damage, or house is displaced
5 (1.0)	**Critical:** Structural integrity fails.	Impact induced collapse, or >50% of building is undercut

Examples of Affected Buildings in Various Damage States

DS1 – Insignificant: Minor non-structural damage

DS2 – Light: Non-structural damage only

DS3 – Moderate: Reparable structural damage

DS4 – Severe: Irreparable structural damage

DS5 – Critical: Structural integrity fails

Disclaimer

A3.4 Building Attributes and Observed Impact from Field Survey

	Building Information											Hazard Information		Rapid Damage Assessment			
No.	Topographic Setting	Age	Footprint (m2)	Foundation	Floor Height (m)	Construction Type	Storey	Wall Cladding	Roof Frame	Roof Slope	Roof Cladding	Landslide Type	Date	Council Placard	Habitability	Estimated Damage	Damage Description
22-1	Sloping ground (Steep, >20°)	1952	351	Concrete rim/ perimeter	0.3	Timber	2	Weatherboard	Timber	Near-flat (1–10°)	Sheet metal	Debris spread/flow	27/09/2022	Y1	Habitable (occupied)	DS1 (0.2); Insignificant: Minor non-structural damage	No obvious damage to the main house, although local/small debris flow observed and debris/trees on top of the roof; no debris got into the house.
22-2	Flat ground, adjacent to slope	2005	260	Concrete slab	0.5	Timber	2	Stucco/ roughcast	Timber	Near-flat (1–10°)	Sheet metal	Debris flow/flood	27/09/2022	R2	Unhabitable	DS5 (1.0); Critical: Structural integrity fails	Level 1 collapsed (due to the accumulated debris in the backyard); foundation looked okay, intact.
22-3	Flat ground, adjacent to slope	1975	172	Concrete slab	0.1	Timber	2	Weatherboard	Timber	Mild (11–30°)	Sheet metal	Retrogressive slump (slippage)	27/09/2022	R2	Unhabitable	DS5 (1.0); Critical: Structural integrity fails	Retaining wall cracked, piles tilted, windows/ doors jammed/stuck; house moved? Instable?
22-4	Sloping ground (Gentle, <10°)	1985	113	Timber pile without brace	0.25	Timber	1	Weatherboard	Timber	Mild (11–30°)	Sheet metal	Rotational slide	27/09/2022	Y1	Habitable (unoccupied)	DS1 (0.2); Insignificant: Minor non-structural damage	No damage to the main house; boat shed destroyed though. No debris got into the house.
22-5	Sloping ground (Gentle, <10°)	1965?	-	Timber pile without brace	1	Timber	1	Weatherboard	Timber	Mild (11–30°)	Sheet metal	Debris flow	28/09/2022	R2	Unhabitable	DS5 (1.0); Critical: Structural integrity fails	Main house collapsed (pushed by lots of debris) and sat on top of garage in the front; sleepout at back was okay. Boat shed at waterfront severely destroyed.
22-6	Sloping ground (Moderate, 10–20°)	2020?	-	Timber pile without brace	0.5-3	Timber	2	Weatherboard	Timber	Mild (11–30°)	Sheet metal	Debris slump/slide (slippage)	28/09/2022	None	Habitable (unoccupied)	DS0 (0); None: No damage	Building intact; lose part of land (in front of house).
22-7	Sloping ground (Steep, >20°)	1970?	-	Timber pile with brace	-	Timber	2	Weatherboard	Timber	Mild (11–30°)	Sheet metal	Debris slump/flow	28/09/2022	Y2	Habitable (unoccupied)	DS2 (0.4); Light: Non-structural damage only	Hit by debris on the side.
22-8	Sloping ground (Gentle, <10°)	1950?	-	Timber pile without brace	-	Timber	1	Weatherboard	Timber	Mild (11–30°)	Sheet metal	Debris avalanche	28/09/2022	R1	Unhabitable	DS3 (0.6); Moderate: Reparable structural damage	Debris hit side of the house, smashed French door; otherwise, the house looked okay.
22-9	Sloping ground (Steep, >20°)	1950?	-	Timber pile without brace	-	Timber	2	Weatherboard	Timber	Mild (11–30°)	Sheet metal	Debris slump/slide (slippage)	28/09/2022	None	Habitable (unoccupied)	DS1 (0.2); Insignificant: Minor non-structural damage	Main house is okay, just lost a bit of foundation.

This page left intentionally blank.

A3.5 Examples of Surveyed Buildings in Various Damage States

DS0 – None: No damage

DS1 – Insignificant: Minor non-structural damage

DS2 – Light: Non-structural damage only

DS3 – Moderate: Reparable structural damage

None

None

DS4 – Severe: Irreparable structural damage

DS5 – Critical: Structural integrity fails

APPENDIX 4 QMAP KEY GROUP NAME DESCRIPTIONS

QMAP – Key Group Name	Description
Caples Terran (Caples T)	Undifferentiated Caples Terrane TZIIA semi-schist
Brook Street Terrane (Brook St T)	Massive to bedded tuffaceous sandstone and siltstone (augite rich basaltic)
Basement melange	Mafic and ultramafic igneous rocks and sedimentary rocks in a sheared serpentinite matrix.
Dun Mountain – Maitai Terrane (Dun Mtn – Maitai T)	Thinly bedded grey sandstone; siltstone; and mudstone with thick green sandstone. Minor siltstone and conglomerate.
Murihiku Terrane (Murihiku T)	Late Triassic? coarse volcaniclastic sedimentary rock, including conglomerate, along the Waimea Fault.
Holocene sediments (H seds)	Well-sorted gravels forming modern flood plains and young fan gravels and inactive dunes.
Pleistocene–Holocene sediments (P–H seds)	Pleistocene–Holocene sediments, including landslide deposits ranging from coherent shattered masses of rock to unsorted fragments in a fine-grained matrix.
Rakaia Terrane (Rakaia T)	Dominantly TZIIIB-IV pelitic schist; derived from quartzofeldspathic sandstone and mudstone.
Waipapa Composite Terrane (Waipapa CT)	TZIIA; weakly to moderately foliated semi-schist
Middle Pleistocene sediments (Mid P seds)	Weathered; poorly sorted to moderately sorted gravel underlying loess-covered, commonly eroded, aggradational surfaces.
Late Pleistocene sediments (Late P seds)	Poorly to moderately sorted gravel with minor sand or silt underlying terraces; includes minor fan gravel.

www.gns.cri.nz

Principal Location

1 Fairway Drive, Avalon
Lower Hutt 5010
PO Box 30368
Lower Hutt 5040
New Zealand
T +64-4-570 1444
F +64-4-570 4600

Other Locations

Dunedin Research Centre
764 Cumberland Street
Private Bag 1930
Dunedin 9054
New Zealand
T +64-3-477 4050
F +64-3-477 5232

Wairakei Research Centre
114 Karetoto Road
Private Bag 2000
Taupo 3352
New Zealand
T +64-7-374 8211
F +64-7-374 8199

National Isotope Centre
30 Gracefield Road
PO Box 30368
Lower Hutt 5040
New Zealand
T +64-4-570 1444
F +64-4-570 4657